HHS Public Access

Author manuscript

Brain Behav Immun. Author manuscript; available in PMC 2023 March 01.

Published in final edited form as:

Brain Behav Immun. 2022 March ; 101: 288–303. doi:10.1016/j.bbi.2022.01.013.

Gestational and lactational exposure to 2,3,7,8-tetrachlorodibenzo-*p*-dioxin primes cortical microglia to tissue injury

R.L. Lowery[1,+], **S.E. Latchney**[1,+,#], **R.P. Peer**[1], **C.E. Lamantia**[1], **K.A. Lordy**[1], **L.A. Opanashuk**[2], **M. McCall**[3,4], **A.K Majewska**[1,*]

[1]Department of Neuroscience, Center for Visual Science, University of Rochester, Rochester, NY 14642

[2]National Institute on Aging, Bethesda, MD 20892

[3]Department of Biostatistics and Computational Biology, University of Rochester, NY 14642

[4]Department of Biomedical Genetics, University of Rochester, NY 14642

Abstract

Recent studies have shown that the aryl hydrocarbon receptor (AhR) is expressed in the brain's native immune cells, known as microglia. However, while the impact of exposure to AhR ligands is well studied in the peripheral immune system, the impact of such exposure on immune function in the brain is less well defined. Microglia serve dual roles in providing synaptic and immunological support for neighboring neurons and in mediating responses to environmental stimuli, including exposure to environmental chemicals. Because of their dual roles in regulating physiological and pathological processes, cortical microglia are well positioned to translate toxic stimuli into defects in cortical function via aberrant synaptic and immunological functioning, mediated either through direct microglial AhR activation or in response to AhR activation in neighboring cells. Here, we use gene expression studies, histology, and two-photon *in vivo* imaging to investigate how developmental exposure to 2,3,7,8-tetrachlorodibenzo-*p*-dioxin (TCDD), a high-affinity and persistent AhR agonist, modulates microglial characteristics and function in the intact brain. Whole cortical RT-QPCR analysis and RNA-sequencing of isolated microglia revealed that gestational and lactational TCDD exposure produced subtle, but durable, changes in microglia transcripts. Histological examination and two-photon *in vivo* imaging revealed that while microglia density, distribution, morphology, and motility were unaffected by TCDD exposure, exposure resulted in microglia that responded more robustly to focal tissue injury. However, this effect was rectified with depletion and repopulation of microglia. These

[*]Corresponding Author: Ania K. Majewska, University of Rochester, School of Medicine and Dentistry, Department of Neuroscience, Center for Visual Science, 601 Elmwood Avenue, Box 603, Rochester, New York 14642, Ania_Majewska@urmc.rochester.edu, Phone: (585) 276-2254.

[#]Present address: Biology Department, St. Mary's College of Maryland, St. Mary's City, MD, 20686

[+]These authors contributed equally to this work

Competing Interests Statement: The authors declare no competing financial interests.

results suggest that gestational and lactational exposure to AhR ligands can result in long-term priming of microglia to produce heightened responses towards tissue injury which can be restored to normal function through microglial repopulation.

Keywords

aryl hydrocarbon receptor; dioxin; two-photon microscopy; microglia; visual cortex; RNA-sequencing; gene expression

1. INTRODUCTION

2,3,7,8-tetrachlorodibenzo-*p*-dioxin (TCDD) is a persistent and exceptionally toxic pollutant and is associated with numerous developmental defects in humans and wildlife (World Health Organization, 2016). Of particular interest, the effects of prenatal TCDD exposure on neurodevelopment are extensively documented, including impaired spatial learning and memory (Markowski et al., 2002), decreased behavioral flexibility and executive functions (Endo et al., 2012; Haijima et al., 2010; Kakeyama et al., 2014), and sex-specific alterations (Ames et al., 2019; Hojo et al., 2002; Ikeda et al., 2005; Nishijo et al., 2012; Tai et al., 2013). Mechanistic studies into these neurobehavioral deficits have revealed abnormal development of the cell layers (Mitsuhashi et al., 2010) and neurons (Nguyen et al., 2013; Xu et al., 2014) that make up the cerebral cortex, a brain region involved in governing higher order brain functions. As a result, these studies have prompted an interest in exploring the cellular and molecular players that contribute to TCDD toxicity in the developing cortex.

Microglia are the immune cells of the brain and their critical roles in mediating brain development have recently been highlighted in a series of studies of the cerebral cortex at different developmental stages (Mendes and Majewska, 2021; Sierra et al., 2019). It is now appreciated that immune deficits and microglial dysfunction accompany many neurodevelopmental disorders including autism spectrum disorder (ASD; (Liao et al., 2020)). Because of the exquisite sensitivity of microglia to their environment, and their critical roles in mediating developmental apoptosis and circuit assembly, these cells may be the nexus that translates toxic developmental insults such as TCDD into aberrant neurodevelopment. TCDD enacts its neurotoxic effects by activating the aryl hydrocarbon receptor (AhR), a ligand-activated transcription factor that plays a large role in sensing environmental conditions (Fallarino et al., 2014; Gu et al., 2000). It was recently shown that constitutive AhR activity during prenatal development negatively impacts dendritic growth and positioning of cortical pyramidal neurons (Kimura et al., 2017b), demonstrating a physiological role for the AhR in regulating cortical development. AhR is widely expressed in the brain (Kimura and Tohyama, 2017) and could affect a large number of targets to disrupt developmental programs, which in turn could affect microglial function indirectly. Additionally, recent reports show that microglia also express the AhR (Ayata et al., 2018; Bennett et al., 2016; Lee et al., 2015; Rothhammer et al., 2018) and microglia AhR activity modulates inflammatory signaling of these cells *in vitro* (Lee et al., 2015) and *in vivo* (Lowery et al., 2021; Rothhammer et al., 2018). There is also evidence *in vitro* that TCDD exposure can increase calcium signaling in microglia which in turn triggers the release of

cytokines and nitric oxide which can damage neurons (Li et al., 2013; Xu et al., 2013), suggesting that direct action of TCDD on microglial AhRs can be neurotoxic. In contrast, however, *in vitro* exposure to formylindolo[3,2-b]carbazole (FICZ), a short-lived AhR agonist, did not elicit an inflammatory response in microglia, unless these cells were primed with lipopolysaccharide (LPS; (Lee et al., 2015)). Additionally, a prior study from our lab found that *in vivo* exposure to TCDD acutely in adulthood did not elicit an inflammatory response in microglia (Lowery et al., 2021). These contradictory results raise the possibility that different AhR agonists may activate AhR signaling in microglia or in other cells to exert different effects on microglia behavior and microglial-mediated inflammation, depending on the inflammatory milieu and timing of exposure (Boule et al., 2018; Lowery et al., 2021; Wheeler et al., 2014). As a result, microglia-mediated neuroinflammation in response to TCDD could negatively impact cortical development and higher order brain functions in a context-specific manner, with timing of exposure being a key variable.

Given the environmental sensing roles of microglia, we hypothesize that the neurotoxic consequences of TCDD exposure on the developing cortex are mediated, in part, by these cells. To test our hypothesis, we examined the effects of gestational and lactational TCDD exposure, hereafter referred to as perinatal exposure, on microglial gene expression and function in the intact brain. Whole cortical gene expression analysis and whole transcriptome analysis of isolated microglia revealed subtle, but durable, changes in gene expression in TCDD-exposed mice. We also found that perinatal TCDD exposure did not alter microglial density, distribution, or morphology, but resulted in microglia that responded more robustly to a focal tissue injury *in vivo*. Furthermore, microglial repopulation following short-term elimination in adolescence (long after direct TCDD exposure had ended) eliminated the TCDD-induced increase in both inflammatory gene expression and pathological response to tissue injury. Our findings indicate that the untimely activation of AhR with TCDD exposure may produce prolonged effects on cortical microglial function that could preclude them from properly responding to tissue injury but that this defective function can be rescued with microglial repopulation.

2. MATERIALS AND METHODS

2.1. Animals.

Experimental protocols were carried out in strict accordance with the University of Rochester Committee on Animal Resources (UCAR) and conformed to the National Institute of Health's "Guide for the Care and Use of Laboratory Animals, 8th Edition, 2011." Two-photon imaging experiments were performed on Cx3cr1GFP/+ mice (Jackson Labs, (Jung et al., 2000)) bred on a C57Bl/6J (Jackson Labs) background which express GFP specifically in microglia in the brain, permitting visualization of microglia *in vivo*. All other experiments were performed on C57Bl/6J mice (Jackson Labs). All mice were exposed to a standard light cycle of 12 hours of light and 12 hours of dark (6AM lights on). Chow and water were provided ad libitum.

2.2. Perinatal TCDD exposure.

The sample size for the experiment examining the impact of perinatal TCDD exposure on microglia baseline characteristics and inflammatory functions consisted of 8 litters of C57Bl/6J mice dosed with olive oil (vehicle) and 8 litters of C57Bl/6J mice dosed with TCDD (500 ng/kg) through oral gavage (Latchney et al., 2013). This dose was chosen because doses <1 μg/kg have been shown to induce changes in synaptic plasticity and developmental neurogenesis in various brain regions including the cortex, hippocampus, and cerebellum (Reviewed in (Latchney and Majewska, 2021)). At least one male and female from each litter were used as a data point, with most data points consisting of data averaged from two males and two females. Pregnant dams were dosed on embryonic day 0 (E0), day 7 (E7), day 14 (E14), and at birth (postnatal day 0; P0), as determined by the presence of a vaginal plug after mating. This dosing schedule (every 7 days until P0) was chosen because the estimated *in vivo* half-life of TCDD in C57Bl/6J mice is 11 days (Gasiewicz et al., 1983) and this is a common dosing paradigm to evaluate perinatal effects of TCDD (Boule et al., 2015; Vorderstrasse et al., 2004, 2006; Winans et al., 2015). Males were removed from the cage once a vaginal plug was observed. For experiments examining *in vivo* process motility and response to laser ablation, individual animals were used as data points. Sample sizes consisted of 4–6 animals per group, with at least 2 males and females per group. A second cohort of animals was generated to examine the impact of microglia repopulation after perinatal TCDD exposure. The sample size of this cohort consisted of 5 litters of C57Bl/6J mice for RNA-seq and 3 litters Cx3cr1GFP/+ mice for *in vivo* imaging and RT-qPCR dosed with either olive oil or TCDD and then given control chow or depletion chow. Data points consisted of individual animals with 5–7 animals per group (2–4 males and females per group).

2.3. Microglia depletion and repopulation.

To eliminate microglia, PLX3397 (290 mg/kg chow PLX3397; Chemgood; Glen Allen, VA; (Elmore et al., 2014)) was formulated in standard mouse chow (AIN-76A-D1001i, Research Diets, New Jersey, USA). At weaning (P21), vehicle- and TCDD-exposed C57Bl/6J and Cx3cr1GFP/+ mice were fed control or PLX3397 chow for two weeks to eliminate microglia then immediately returned to standard control chow for an additional two weeks to allow microglia to fully repopulate. Depletion was verified in littermates sacrificed immediately following the depletion period. Significant depletion was achieved with 97.4% of microglia eliminated in PLX3397-treated animals (n=4; 2 males, 2 females) compared to controls. Immediately following microglia repopulation, cortical inflammatory state was assessed with RT-QPCR (C57Bl/6J) and microglia function was assessed with two-photon imaging (Cx3cr1GFP/+).

2.4. Gene expression analyses.

RNA was extracted using the RNeasy Mini Plus kit (Qiagen) according to the manufacturer's instructions. RNA was quantified using the Nano Drop spectrophotometer. 1 μg of RNA was reverse transcribed to cDNA using Superscript IV reverse transcriptase and random hexamers (Invitrogen). To test that RNA was free of genomic DNA contamination, a control without reverse transcriptase was included.

Real-time quantitative polymerase chain reaction (RT-qPCR) analysis was conducted using an Applied Biosystems QuantStudio 3 Real-Time PCR system with the following reaction set-up: 5 μL of Power SYBR Green PCR Master Mix (Applied Biosystems), 0.08 μL of reverse and forward primers each (20 μM), 3.84 μL of RNase-free water, and 1 μL of cDNA (5 ng). A water-only control was also included in each reaction. The qPCR cycling conditions were: 50°C for 2 minutes, 95°C for 10 minutes, followed by 40 cycles of 95°C for 15 seconds and 60°C for 1 minute. Optimization of primer concentrations and primer efficiencies using a 5-log dilution series was carried out prior to the commencement of quantification experiments. Only primer sequences and cycling conditions that yielded primer efficiencies between 90 and 110% were used. Samples were set up in duplicate and analyzed using QuantStudio design and analysis software (Applied Biosystems). Melt curve analysis was also performed on all samples. Calculations used the comparative C_T ($\Delta\Delta C_T$) method (Livak and Schmittgen, 2001) and measurements were normalized to the expression of three reference genes, Gapdh, β-actin, and Eif2b1. Primer 3 software was used to design exon-spanning primers and sequences are listed in Table 1.

2.5. Microglial isolation by fluorescence activated cell sorting (FACS).

Male and female C57BL/6 mice at ages P28 to P34 were processed for FACS and RNA-seq as described previously (Stowell et al., 2019; Wong et al., 2018). Mice were euthanized by intraperitoneal injection of sodium pentobarbital (Euthasol, Virbac, St. Louis, MO) and transcardially perfused with ice cold 0.15 M PB. Each brain was removed and the cortex was immediately dissected in ice-cold, degassed FACS buffer (0.5% BSA (Sigma A2153) in 1X PBS without cations (Invitrogen 20012–027 pH 7.2).

Tissue was kept on ice and dissociated into a single-cell suspension with a Dounce homogenizer. Dissociated cells were passed through a 70 μm filter and centrifuged at 274 x g for 7 minutes at 4°C. Supernatants were removed and cell pellets were prepared for magnetic labeling with Myelin Removal Beads II according to the manufacturer's instructions (Miltenyi 130–0960733). Magnetic columns (Miltenyi 130–096-733) were primed with FACS buffer and samples were applied to the columns through a clean 70 μm filter. The myelin-depleted flow-through was centrifuged, the supernatant removed, and the cell pellets incubated in Fc block (BioLegend 101320) for 15 minutes at 4°C.

Following Fc block, cells were protected from light and incubated with CD11b-Alexa Fluor 488 (Clone M1/70; BD Pharmingen 557672) and CD45-APC (Clone 30/F11; BD Pharmingen 561018) for 30 minutes at 4°C. Compensation controls (Alexa Fluor-488 beads, APC beads (eBiosciences 01–111-42), unstained cells, and triton-X treated cells) were also prepared fresh. DAPI was used to discriminate live/dead cells (Molecular Probes; final concentration: 2 μg/mL). All samples and controls were re-suspended in 400μL of FACS buffer with DAPI just prior to sorting on an 18-color FACS Aria II flow cytometer (BD Biosciences). Our ability to specifically isolate microglia with this FACS protocol was validated by examining the relative transcript expression levels of a subset of genes of interests divided into three groups (Wong et al., 2018): Group 1) genes expressed solely in CNS microglia, Group 2) genes expressed differentially in immunologically reactive CNS microglia, and Group 3) genes expressed in neurons, astrocytes, and oligodendrocytes

(Supp. Figure 1). Microglia specific genes such as Cx3cr1, P2ry12, and Tmem119 had consistently high expression while genes expressed in cells other than microglia such as Thy1, S100ß, and Mog had consistently low expression, demonstrating the specificity of our microglia FACS-sorting protocol. Furthermore, markers of peripheral immune cells Cd19 (B cells), Cd3E (T cells), and Ly6G (granulocytes) were not detected, demonstrating that the FACS-sorted samples did not contain peripheral immune cells (Grabert et al., 2016; Wong et al., 2018).

2.6. RNA isolation and RNA-sequencing.

Total RNA from sorted microglia (CD11b+, CD45-low) was isolated using the RNeasy Micro Kit (Qiagen). RNA Integrity Number (RIN) was 9.38 ± 0.2 and RNA concentration was 590 pg/μL ± 0.07 across the 20 samples. 1 ng of total RNA was pre-amplified with the SMARTer Ultra Low Input kit v2 (Clontech; (Wong et al., 2018)). cDNA quality was determined using a Qubit Flourometer (Life Technologies) and Agilent 2200 TapeStation. Illumina compatible sequencing libraries were generated from 5 ng cDNA with the NexteraXT library prep kit (Illumina). Libraries were hybridized to the Illumina single-end flow cell and amplified using the cBot (Illumina) at 8 pM per lane. Single-end reads of 100nts were generated. Data analysis included adapter removal by Trimmomatic-0.36 “TRAILING:13 LEADING:13 ILLUMINACLIP:adapters.fasta:2:30:10 SLIDINGWINDOW:4:20 MINLEN:35” (Bolger et al., 2014). Mapping to the mouse reference genome (GRCm38.p4) with done using STAR 2.6.0c a “--twopassMode Basic --runMode alignReads --genomeDir ${GENOME{ -readFilesIn ${SAMPLE} --outSAMtype BAM SortedByCoordinate --outSAMstrandField intronMotif --outFilterIntronMotifs RemoveNoncanonical” (Dobin Bioinformatics 2013). Read quantification was accomplished with HTSeq-count v0.6.1 “subread-1.6.1, featurecounts, -s 0 -t exon -g gene_name” and “subread-1.6.1, featurecounts, -M -s 0 -t exon -g gene_name.” Identification of differentially expressed genes was completed using DeSeq2–1.16.1.

The 12,167 genes found to be expressed (read counts > 50) in at least one sample were retained for subsequent analyses. Linear modeling was performed using the limma R package (version 3.44.3) with precision weights calculated using voom (Law et al., 2014). The linear model for each gene contained binary indicator variables for TCDD exposure and sex and an interaction between TCDD exposure and sex. Gene set testing was performed using ROAST (Wu et al., 2010), which implements a rotation-based allowing for gene-wise correlation.

2.7. Histology.

Brains were harvested from gestationally-exposed mice at P28. All mice were first deeply anesthetized using Euthasol, perfused intracardially with 0.1 PBS with heparin and 4% paraformaldehyde. Brains were removed and cryoprotected using a graded sucrose treatment (10% and 30%). Coronal sections were taken at 50 μm thickness using a standard freezing microtome and stored in cryoprotectant (25% 0.2M PBS, 25% glycerol, 30% ethylene glycol, and 20% distilled water). Sections that included the primary visual cortex (V1) were selected for histological processing and were level-matched to exclude the impact of regional differences in microglia density and morphology. V1 was chosen as microglia are

known to be critical mediators of synaptic plasticity in developing V1 (Sipe et al., 2016; Stowell et al., 2019) and AhR deletion leads to functional deficits in V1 neuronal circuitry (Juricek et al., 2017).

Sections were processed free-floating at room temperature (RT), except where noted. Briefly, sections were rinsed in 0.1M PBS, incubated in a 10mM sodium citrate buffer at 80°C for 30 minutes, and brought to RT before rinsing in 0.1M PBS. Sections were then incubated in a peroxidase block (10% Methanol, 30% Hydrogen Peroxide) for 20 minutes, rinsed in 0.1 PBS, and transferred to an additional blocking solution (0.2% Triton-X, 5% Bovine Serum Albumin) for one hour. After this block, sections were incubated for 24 hours in a humidified chamber at 4°C in primary antibody (1:2500 rabbit polyclonal anti-Iba-1, Wako Pure Chemical Industries Inc. #019–19741; 0.5% Bovine Serum Albumin). Sections were allowed to acclimate to RT for 30 minutes and subsequently incubated for 4 hours in secondary antibody (1:500 donkey anti-rabbit Alexa Fluor 488, Invitrogen, Catalogue# A21206; 0.5% BSA), followed by a final rinse in 0.1 PBS and then mounted onto slides with Prolong Gold Mounting Media (Invitrogen; #P36934).

2.8. Image Analysis.

Histologically processed sections were imaged using a standard confocal microscope (Zeiss LSM 510 META) with 20x, 0.5 NA, air-immersion and 40x, 1.2 NA, water-immersion objectives at a digital scan resolution of 1024 X by 1024 Y. For all animals, images were taken of three different sections of V1 with the exception of three animals in which images of only two sections could be taken due to tearing. Images were then imported into Image J and projected in the z dimension.

2.8.1. Microglial Density Analysis: Images containing white matter were cropped to include only V1. Each microglial cell body was marked, and the number of microglia and their coordinates were recorded. The number of microglia was used to determine cellular density (number of microglia/mm^2). The average cellular density was then taken for each litter.

2.8.2. Microglial spacing analysis: The cellular coordinates obtained in ImageJ were analyzed using a custom algorithm implemented in Matlab (Mathworks) in order to determine the average distance between each microglia and its nearest neighbor (nearest neighbor distance). A spacing index was generated as: (average nearest neighbor distance)^2 * microglial density. The average spacing index was then taken for each litter.

2.8.3. Sholl analysis: Sholl Analysis was conducted with an automated ImageJ Sholl analysis plugin (kindly provided by the Anirvan Ghosh Laboratory, UCSD) in order to determine the level of ramification of the microglia. This was done by drawing concentric circles starting at a radius equivalent to that of the microglial soma and increasing in radius size by a constant value of 2μm. The number of intersections between the circles and microglia branches was counted and used to determine the branching density of microglia as a function of distance from the soma. For quantitative analysis between groups, the

maximum number of intersections was calculated, along with the full width at half max (estimated by interpolating the data points on the Sholl graphs for each animal).

2.9 Two-Photon Imaging.

In vivo imaging was performed using a custom two-photon laser-scanning microscope. The microscope consists of a Ti:Sapphire laser providing 100 femtosecond pulses at 80MHz at a wavelength of 920nm (Mai Tai, Spectra-Physics) and a modified Fluoview confocal scan head (Olympus). For single channel imaging of GFP, fluorescence was detected using a photomultiplier tube (Hamamatsu) and a 580/180 filter. Image acquisition was accomplished using a 20x, 0.95 NA lens (Olympus) and Fluoview software. All imaging was carried out on gestationally-exposed animals when they were between P60 and P600. Mice were anesthetized with fentanyl cocktail [fentanyl (0.05 mg/kg), midazolam (5.0 mg/kg), and dexmedetomidine (0.5 mg/kg), i.p.] and body temperature was maintained at 37°C.

For quantification of microglia motility, an area of the skull was thinned over primary visual cortex (V1) in adult Cx3Cr1GFP/+ mice exposed gestationally to either TCDD or saline. Z-stack images of microglia were collected at digital zoom 5, every 5 minutes for one hour. Analysis was performed offline in ImageJ and Matlab using custom algorithms. Z-projections of consistent depth were generated for each time interval, concatenated, and corrected for motion artifact. A threshold was applied to all images, and color overlays generated for adjacent sets of time points, resulting in a single image where magenta pixels represent processes present in only the first time point (retraction), green pixels represent processes present in only the second time point (extension), and white pixels represent processes present in both adjacent time points (stability). A custom Matlab algorithm (Sipe et al., 2016) was used to compare pixels across time points or across overlays and generate a motility index (defined as the sum of all magenta and green pixels divided by all white pixels), a stability index (defined as the proportion of green pixels that became white in a subsequent overlay), and an instability index (defined as the proportion of white pixels which became magenta in a subsequent overlay). For each index, individual microglia values were averaged to generate the value per animal.

2.10. Focal laser ablations.

Laser ablations were achieved by carrying out a point scan localized at a microglial cell body for 15s at 780 nm using ~75mW at the sample. The microglial response to laser ablation was assayed as described previously (Davalos et al., 2005; Sipe et al., 2016), by quantifying the movement of microglial processes entering an inner radius (X, 1.75x ablation core diameter) centered around the ablation from an outer radius (Y, 3.0x ablation core diameter) over time. Timelapse z-projection images were generated and thresholded to normalize background fluorescence. The total number of pixels in X and Y were measured across time [Rx(t); Ry(t)] and the ablation response was calculated using the equation $R(t)=(Rx(t)-Rx(0))/Ry(0)$. For quantitative analysis, the maximum response and the time taken to half of the maximum response was calculated from individual response graphs.

2.11. Statistical Analysis.

Statistical analysis was conducted using the GraphPad Prism 6 statistical software. All data is shown as the mean ± standard error of the mean (SEM) and significance was determined using $\alpha < 0.05$. The Grubbs Outlier test (http://graphpad.com/quickcalcs/Grubbs1.cfm) was used to check for and exclude statistical outliers (1 outlier removed from Figure 2 TNF-α comparison). For all comparisons of animals exposed to either TCDD or vehicle during gestation using data combined for both sexes, two-tailed, unpaired student t-tests were used to determine significance. For sex-specific effects and effects of repopulation, significance was determined using two-way ANOVAs with Bonferroni multiple comparisons tests.

3. RESULTS

3.1. Pro- and anti-inflammatory cytokines are increased in P28 cortex of TCDD exposed mice.

To understand how microglia are impacted by perinatal TCDD exposure, we exposed pregnant dams with TCDD or vehicle at embryonic day 0, 7, 14 and again at birth, simulating prolonged exposure during development through both gestational and lactational routes (Figure 1A). This exposure paradigm resulted in a 17% decrease in whole body weights of the TCDDexposed offspring vs. vehicle-exposed offspring Figure 1B; unpaired t-test, $P = 0.0002$;). When analyzed by sex, only TCDD-exposed males had significantly reduced body weights compared to their vehicle equivalents (Figure 1C; two-way ANOVA, exposure: $P < 0.0001$; Bonferroni post-hoc test $P < 0.0001$). Interestingly, TCDD-exposed mice exhibited a 12% increase in cortical brain weight (Figure 1D; unpaired t-test, $P < 0.0001$). This weight increase was evident in both TCDD-exposed females and males, with TCDD-exposed males exhibiting more significant cortical weight gain than TCDD-exposed females (Figure 1E; two-way ANOVA, exposure: $P < 0.0001$; Bonferroni post-hoc test female: $P = 0.0114$, male: $P = 0.0026$). To confirm the action of TCDD in the brain, we performed RT-qPCR to assay expression of the AhR downstream target gene Ahrr. We found a significant increase in Ahrr expression (Figure 1F,G; unpaired t-test, $P = 0.0150$) demonstrating that TCDD successfully activates the AhR signaling pathway following this perinatal TCDD exposure paradigm.

To assess whether perinatal TCDD exposure creates an inflammatory environment in the brain, we quantified the gene expression of several pro- and anti-inflammatory cytokines in the whole cortex (Figure 2). While gene expression does not necessarily reflect protein expression, TCDD-exposed mice had a small, but significant, increase in several cytokines, including TNF-α, IL-6, IL-1β, iNOS, and Arginase compared to vehicle-exposed mice (Figure 2; Table 2; unpaired t-test, TNFα: $P < 0.0001$; IL-6: $P = 0.0045$; IL-1β: $P < 0.0001$; iNOS: $P = 0.0236$; Arg: $P = 0.0080$). These cytokines have previously been shown to be secreted by microglia (Cherry et al., 2015; Lee et al., 2015; Li et al., 2013; Xu et al., 2013). When analyzed by sex, only the TCDD-exposed males exhibited a significant increase in pro- and anti-inflammatory cytokines compared to their vehicle-exposed equivalents (Figure 2; Table 2; two-way ANOVA/Bonferroni post-hoc, TNFα: sex: $P = 0.8159$, post-hoc: $P = 0.0001$; IL-6: sex: $P = 0.0004$, post-hoc: $P < 0.0001$; IL-1β: sex: $P = 0.6248$, post-hoc: $P =$

0.0005; iNOS: sex: $P = 0.0845$, post-hoc: $P = 0.0018$; Arg: sex: $P = 0.2725$, post-hoc: $P = 0.0093$).

To determine the contribution of specifically microglia in modulating neuroinflammation following perinatal TCDD exposure, we used fluorescence activated cell sorting (FACS) to isolate microglia from the cortex at P28 and RNA-sequencing to assess changes in the transcriptome of these microglia (Figure 3; Supplementary Figure 1). To assess perinatal TCDD-related changes in the microglial transcriptome, we performed RNA-sequencing on these FACS-isolated microglia. When looking at individual genes, after adjusting for multiple testing, we found no adjusted p-values less than 0.05. However, there were 346 genes with a logfc greater than or equal to 1.5, indicating that some genes were affected by TCDD in these samples, and the number of affected genes and direction of change differed between males and females (Figure 3). These findings indicate that the FACS procedure may have altered what may have already been a mild phenotype by causing overall mild reactivity and are consistent with our initial findings in Figure 2 in that perinatal TCDD exposure may produce subtle, rather than profound, changes in microglial transcript expression.

3.2. Changes in microglial morphology and dynamics are not evident in mice developmentally exposed to TCDD.

To determine whether perinatal exposure to TCDD causes a lasting defect in microglial function, we examined the immunoreactivity of Iba-1, a microglial marker, in fixed sections of visual cortex at P28. Because microglia infiltrate the brain during embryogenesis, we first examined the recruitment and establishment of microglia by quantifying the density and spacing of microglia in primary visual cortex. Cortices from both exposure groups were tiled with Iba-1 positive microglia that appeared evenly spaced across the whole region (Figure 4A), and we found no significant difference between the vehicle and TCDD exposed groups in regards to microglial density (Figure 4B). In addition, we found no significant difference in their spacing index, which quantifies the regularity of microglial placement given their density in the cortex (Figure 4C). This suggests that perinatal TCDD exposure does not cause an overt developmental defect in microglial ability to populate and distribute within cortical regions of the brain. We also looked for any sex-specific differences in density or spacing of the two groups, since it has been suggested that both baseline and toxicant-elicited sex-specific differences in microglial behavior exist (Bolton et al., 2017; Lenz et al., 2013; Schwarz et al., 2012), and we have observed a sex-specific difference in TCDD-induced inflammation (Fig. 2). We found that microglia from male and female vehicle-exposed mice showed similar densities and spacing characteristics (Figure 4D–E). While TCDD exposure did not alter density or spacing in female mice, TCDD-exposed males have microglia which are significantly more clustered compared to males developmentally exposed to oil, although the effect was small at about 10% change (Figure 4E; two-way ANOVA, $P = 0.0291$; Bonferroni post-hoc test, $P < 0.01$). This implies that perinatal TCDD exposure has limited effects on microglial density and distribution long-term.

While our density, spacing, and gene expression analysis did not suggest overt reactivity, we decided to analyze microglial morphology using Sholl analysis, which quantifies microglia ramification by analyzing arbor complexity to look at subtle changes that might be indicative of an altered microglial state (Figure 5A), since more reactive microglia typically have less branching and arbor complexity (Kettenmann et al., 2011). Both qualitative analysis of the images and the Sholl quantification showed similar branching of microglia in the two conditions (Figure 5B–C), with the arbor becoming most complex at a distance of 12 μm away from the soma with ~15 intersections occurring at this distance. Arbors had a radius of ~40 μm in both conditions. We did not find any significant effect of perinatal TCDD exposure on the maximal height or full width half max of the curve of the Sholl curve (Figure 5E–F). We also separated out male and female mice and found that there was no significant effect of sex in vehicle- or TCDD-exposed mice (Figure 5D, G–H).

Because physiological microglia are highly motile (Davalos et al., 2005; Nimmerjahn et al., 2005) and it is likely that this behavior is required for the role microglia play in mediating neurophysiological processes, we assayed microglial process motility *in vivo* in adult mice in the presence or absence of perinatal TCDD exposure (Figure 6A). We found that perinatal TCDD exposure had no effect on microglial process motility (a measure which includes retraction and extension; Figure 6B), stability (a measure of stabilization of newly extended processes; Figure 6C), or instability (a measure of retraction of previously stable processes; Figure 6D). These results suggest that perinatal TCDD exposure does not have a long-lasting impact on microglial dynamic behavior. We also separated out male and female mice and, while the small sample size precluded rigorous analysis, there were no apparent trends that suggest sex-specific differences in motility, stability, or instability in vehicle or TCDD exposure conditions (Figure 6E–G).

3.3. Microglial priming to tissue injury is evident in mice developmentally exposed to TCDD.

While perinatal TCDD exposure did not cause overt changes in baseline microglia characteristics, such exposure may impact the ability of microglia to respond to a pathological stimulus (Norden et al., 2015). To determine the impact of perinatal TCDD exposure on the microglial response to pathological insult, we performed a laser ablation to assay the microglial response to a focal brain injury *in vivo* (Figure 7A). We found there was a significant increase in the magnitude, but not the speed, of the microglial response to a focal injury in TCDD versus vehicle-exposed adult mice (Figure 7B–D, Student's t-test, $p = 0.0377$). No sex-specific effects were apparent (Figure 7E,F). These results suggest that while perinatal TCDD exposure may not induce detectable differences in baseline microglia behavior, it may influence how microglia respond to cortical injury.

3.4. Short-term microglia depletion and repopulation.

Healthy (Elmore et al., 2014) and injured (Rice et al., 2017; Rice et al., 2015) microglia require signaling from the colony-stimulating factor 1 receptor (CSF1R) for their survival. Small-molecule CSF1R inhibitors have been shown to cross the blood brain barrier and rapidly eliminate microglia (Elmore et al., 2014). Subsequent withdrawal of CSF1R inhibitors from microglia-depleted mice results in rapid repopulation with new microglia

within 14 days (Bruttger et al., 2015; Elmore et al., 2014). We hypothesized that microglia depletion would reverse the TCDD-induced increase in cortical inflammation. To test this hypothesis, Cx3cr1GFP/+ mice exposed to vehicle or TCDD were fed control or PLX3397 chow starting at P21 for two weeks to eliminate microglia then immediately returned to standard chow for an additional two weeks to allow microglia to fully repopulate (Figure 8A,B). Following microglia repopulation, RT-QPCR was used to assay cortical inflammatory environment and two-photon imaging was used to survey microglia function. We again found a significant increase in several cytokines, including TNFα, IL-6, IL-1β, iNOS, and arginase, as a result of TCDD exposure alone (Figure 8C; Table 2; two-way ANOVA/Bonferroni post-hoc test, TNFα: repopulation: $P = 0.3386$; post-hoc: $P = 0.0031$; IL-6: repopulation: 0.0088, post-hoc: $P < 0.0001$; IL-1β: repopulation: $P = 0.0014$, post-hoc: $P < 0.0001$; iNOS: repopulation: $P = 0.0315$, post-hoc: 0.0080; Arg: repopulation: $P = 0.0023$, post-hoc: $P < 0.0001$). However, there was no significant difference between either vehicle control or vehicle repopulated conditions and the TCDD-exposed repopulated condition (Figure 8C), indicating that microglial repopulation rectifies the inflammatory milieu induced by perinatal exposure to TCDD. Similarly, two-photon imaging indicated that while there is no difference in microglial process motility across conditions (Figure 9A), this cohort again exhibited an increased inflammatory response to focal tissue injury as a result of TCDD exposure alone (Figure 9B; two-way ANOVA, exposure: $P = 0.3139$; Bonferroni post-hoc test, $P = 0.0232$). Moreover, there was no significant difference between either vehicle control or vehicle repopulated conditions and the TCDD-exposed repopulated condition (Fig 9B), indicating that microglial repopulation rectifies the aberrant pathological response to tissue insult induced by perinatal exposure to TCDD.

4. DISCUSSION

This study provides *in vivo* evidence that microglia in the intact brain may be uniquely positioned to translate toxic stimuli resulting from developmental TCDD exposure into long-term deficits in cortical brain functions. Our results suggest that, similar to acute, adult TCDD exposure (Lowery et al., 2021), perinatal exposure to TCDD does not cause overt changes in microglia that would indicate a severe deficit in the development of this immune cell, despite creating an inflammatory environment that is more evident in males. We found no defect in microglial ability to properly infiltrate the brain, establish distinct territories, develop a ramified morphology, and surveil the local environment via process motility. However, analysis of the microglia transcriptome revealed subtle, but durable, changes in microglial transcripts that, in their sum, could prime microglia to mount a pathological response to tissue injury. Indeed, we found that microglia exposed to TCDD perinatally respond more robustly to focal tissue injury. Encouragingly, both neuroinflammatory signaling and the related functional microglial defects could be rectified by depletion and repopulation of microglia at a time point after direct TCDD exposure had ceased. This suggests that microglia may mediate long-term effects of TCDD toxicity in the brain and can be targeted therapeutically. Below we discuss possible interpretations of these data, and the implications for future research on AhR agonists and CNS immune cells.

4.1. Responsiveness of CNS vs. peripheral immune cells following developmental TCDD exposure

Within the peripheral immune system, TCDD exposure leads to immunosuppression (Mandal, 2005), a process that is mediated via the AhR (Fernandez-Salguero et al., 1995). Given that microglia express AhR (Ayata et al., 2018; Bennett et al., 2016; Lee et al., 2015; Rothhammer et al., 2018), we expected a similar defect in the development of these immune cells. However, we found no evidence for a change in the state of microglial cells and microglia were able to divide, colonize the brain and transition into mature, ramified morphologies from immature infiltrating cells. Genomic analyses did not uncover large changes in microglial expression patterns that would indicate immunosuppression or altered maturation. This may suggest that microglia are relatively protected from TCDD exposure as compared to peripheral immune cells. One possible explanation for this contrasting vulnerability to TCDD is the considerable variability in AhR signaling in different immune cell populations. For example, while TCDD exposure leads to thymic involution and decreased T cell maturation (Vos et al., 1997), natural killer cell activity was found to be resistant (Kerkvliet, 1995). Similarly, while some groups have found that absence of the AhR leads to defective immune cell development, as evidenced by decreased T-cell and T-helper 17 cell development (Quintana et al., 2008; Stevens et al., 2009), other groups have found that there is no defect in functional immune response despite loss of the receptor (Vorderstrasse and Kerkvliet, 2001; Vorderstrasse et al., 2001). Taken together, these studies suggest that the impact of TCDD exposure on immune cell populations is cell-type dependent.

4.2. Direct vs. Indirect effects of TCDD on microglia

The subtle phenotype of TCDD-exposed microglia may be the result of the relative expression levels of AhR in microglia compared to other brain cell types in the mouse cerebral cortex. A RNA-sequencing study demonstrated that while cortical microglia express AhR, the expression level is much less than that in neurons, astrocytes, and endothelial cells (Zhang et al., 2014), and our RNA-seq results in FACS-sorted microglia are consistent with this low baseline expression. AhR deletion in brain Cx3Cr1+ cells induces an inflammatory microglial phenotype and acceleration of experimental autoimmune encephalitis (Rothhammer et al., 2018), showing that AhR is active in microglia and/or brain macrophages in the setting of adult disease. However, in the absence of tissue injury or an inflammatory environment, microglia may be relatively resistant to AhR ligands compared to other brain cell types, as observed in our prior study of adult TCDD exposures (Lowery et al., 2021), especially considering that AhR-null mice are resistant to the toxic effects of TCDD (Boule et al., 2018; Latchney et al., 2013; Winans et al., 2015). In line with this, *in vitro* exposure to 6-formylindolo[3,2-b]carbazole (FICZ), a shortacting AhR agonist with a very different metabolic profile than TCDD, alone was also not sufficient to activate AhR in freshly isolated microglial cells, but could activate AhR in astrocytes (Lee et al., 2015). While this could partially be explained by higher AhR transcript expression in astrocytes than in microglia (Zhang et al., 2014), the contrasting responsiveness may suggest distinctive and characteristic functions for microglial vs. astrocyte AhR in mediating neuroimmune responses, which remain to be explored. The low expression of AhR in microglia at baseline may elicit differential microglial responses to different AhR ligands, or

these low levels may preclude a direct effect of some AhR ligands on microglia, promoting instead a microglial response to AhR activity in cell types with higher AhR expression. Indeed, our results suggest that the effects of TCDD on microglia may be indirect because we found that perinatal TCDD exposure did not significantly alter Ahrr gene expression in sorted microglia while it did significantly increase Ahrr expression in whole brain tissue. There is also a chance TCDD exposure induces an acute short-lasting activation of microglial AhR that was no longer present at P28 when we assayed Ahrr. AhR is expressed throughout the brain (Kimura and Tohyama, 2017), and microglial surveillance allows microglia to monitor many different cell types through diffusible signaling and direct physical contacts. Thus, narrowing down indirect effects of TCDD and AhR activity on microglia will be challenging. One likely target for TCDD could be proliferating neural progenitor cells as TCDD exposure has been shown to alter multiple stages of developmental neurogenesis including neural progenitor cell proliferation, differentiation, and migration and these effects are heavily dependent on the ligand used to activate the receptor, the dosing regimen, brain region analyzed, and the age and timing of exposure (Collins et al., 2008; Dever et al., 2016; Kimura et al., 2017a; Kolluri et al., 1999; Mitsuhashi et al., 2010; Wei et al., 2021; Williamson et al., 2005). It is conceivable that effects on developmental neurogenesis could lead to changes in cortical structure and ultimately influence behavior (Reviewed in (Latchney and Majewska, 2021)). Therefore, since there are no significant changes in microglia number and density, the increase in cortical weight observed in TCDD-exposed mice is unlikely derived from microglial changes and instead could be due to abnormalities in neurogenesis. It is interesting to note that forced repopulation of microglia, which replaced the microglial niche with microglia that had not been exposed to TCDD, normalized microglial behavior. This suggests that TCDD may indeed have subtle direct effects on microglia or that indirect effects are also restricted to the time period of TCDD exposure.

4.3 Context-dependent effects of TCDD on microglia

As suggested above, it is possible that an inflammatory cellular milieu may be required for microglia to respond to AhR ligands. Prior studies in peripheral (Vorderstrasse et al., 2004; Winans et al., 2015) and CNS (Lee et al., 2015) immune cells have consistently shown that exposure to short- or long-acting AhR agonists does not stimulate a robust immune response on its own, unless these immune cells are exposed to an inflammatory stimulus Consistent with these studies, we also find that *in vivo* microglial function is not altered with TCDD exposure unless these cells are presented with a focal tissue injury. The increased reactivity of TCDD-exposed microglia to tissue injury could be due to a primed transcript profile in these cells (Norden et al., 2015), as we did see some non-significant changes in our expression studies. Whether these altered transcripts and altered microglial responses lead to deficits in higher brain functions involving the cortex also remain to be explored. Inflammation can also upregulate AhR expression in microglia (Lee et al., 2015), adding to the context-dependent responsiveness of microglial AhR. AhR upregulation can make microglia more susceptible to toxic AhR ligands like TCDD when these microglia are immunologically challenged. When combined with these previous reports, our findings add to the emerging model that microglial AhR may be resistant to individual insults (Lowery

et al., 2021; Vorderstrasse et al., 2004; Winans et al., 2015), but may prime microglia to be more susceptible to secondary stimuli (Norden et al., 2015).

An additional question is whether other contexts could also uncover latent microglial deficits. Microglia are critical to many physiological brain functions and can mobilize phagocytic machinery and undergo morphological alterations during periods of intense synaptic remodeling (Mendes and Majewska, 2021). Recent research elucidating the intertwined nature of microglia pathological and physiological functions suggests that chronic, microglia-mediated inflammation shifts the balance away from physiological functions towards pathological functions resulting in a loss of normal microglia-mediated physiological processes (Perry and Holmes, 2014; Shahidehpour et al., 2021). Thus it is possible that in the presence of plasticity-inducing stimuli TCDD-exposed microglia may likewise show deficits in mounting an appropriate response.

4.4. Sex-dependent effects following perinatal TCDD exposure

There is increasing evidence defining sex-dependent differences in microglia both under physiological (Guneykaya et al., 2018; Hanamsagar et al., 2017) and pathological conditions, including in response to environmental insults (Bolton et al., 2017). In line with this, we found a sexually dimorphic inflammatory response to TCDD exposure with TCDD-exposed males demonstrating a mild, but significant, upregulation in inflammatory cytokines. Additionally, while we did not find a significant effect of sex on microglial gene expression profiles following TCDD exposure, we did observe a different pattern of gene regulation in TCDD-exposed microglia from male and female mice. However, converse to our gene expression findings, we did not find any overt and persistent sex-specific effects of TCDD exposure on either baseline microglia characteristics or response to tissue injury. Given recent literature suggesting that male and female microglia proceed along the path of developmental programming on different timescales (Thion et al., 2018) which subsequently renders male microglia more susceptible to disruptions during development, it is possible that the gene expression changes in TCDD-exposed males were not large enough to translate to male-specific changes in microglia behavior. Limited data examining sex in microglial studies makes interpretation of sex-specific differences in microglial behavior difficult and underscores the need for increased inclusion of sex as a variable in future studies.

4.5 Microglia repopulation and rescue of developmental environmental exposure-induced defects

Removing TCDD-exposed microglia and replacing them with naïve microglia, using depletion and repopulation techniques, resulted in the resolution of the whole brain inflammatory milieu and restoration of normal microglial functional response to acute tissue injury. These findings suggest that microglia are responsible for the TCDD-induced inflammatory signaling and may propagate their own immune deficits rather than responding to prolonged changes in other cells. This also shows that defects resulting from environmental insults that occur during early life, a sensitive period of microglial development, are not permanent and can be rectified at a later time. Whether the effects of repopulation are long-lasting, however, is not clear. In the aged brain, microglial depletion and repopulation resulted in new, replenished microglia that morphologically

resembled young, un-primed microglia and age-related neuronal and cognitive defects were reversed (Elmore et al., 2018). However, this microglial rejuvenation only partially reversed the primed, aged phenotype due to continued exposure to an unchanged inflammatory environment in the aged brain (O'Neil et al., 2018). These findings underscore the importance of the brain microenvironment in influencing microglial function and suggest the importance of examining later time points in our model to assess whether the continued presence of TCDD in fatty tissue or long-lasting changes in other cortical cells could act as a continued insult that would return newly born microglia to their previous state.

It is puzzling that repopulated microglia appear to have restored function given that microglial repopulation is thought to proceed from a small number of microglia that remain through the depletion process. There are at least two possible explanations for this finding. First, it is possible that while the parent microglia were negatively impacted by TCDD exposure either directly or through interactions with other cell types at the time of TCDD exposure, the resulting defect is not passed to the daughter cells. This may be due to the lack of epigenetic or cytoplasmic changes that would be passed to daughter cells and may be insult-specific. Second, it is possible that the subset of microglia which remain after Csf1R-inhibition may be a distinct population that is more resistant to external insults. Recent research suggests that there is a CSF1R-independent population of microglia which are highly proliferative and seem likely to be the population remaining following depletion via Csf1R inhibition (Mendes et al., 2021; Zhan et al., 2020). This subset of microglia, which distinctly express Mac2, may likewise respond differently to outside insult. While this remains to be tested experimentally, mounting evidence supports the idea that microglia are a highly heterogeneous population (Masuda et al., 2020), and if true, this would allow a common strategy for rejuvenating microglia after different insults.

4.6. Conclusion and future outlook

It is important to continue probing the impact of TCDD exposure on CNS immune cells. Because AhR activation may positively influence peripheral immune cell development, the use of AhR ligands has been proposed as a potential therapeutic option for immune-related disorders (Barroso et al., 2021; Marshall and Kerkvliet, 2010). However, it has recently been demonstrated that exposure to AhR agonists such as dietary tryptophan metabolites induces wildtype microglia to take on the same inflammatory phenotype as AhR-null microglia (Rothhammer et al., 2018). These findings suggest that while AhR manipulation may have peripheral benefits, it may not be beneficial in the CNS and underscores the importance of further elucidating the role of AhR and its binding partners in microglial function and their neuromodulatory roles in development (the current study) and adulthood (Lowery et al., 2021). Here, we expand on our prior study (Lowery et al., 2021) and demonstrate that microglia are indeed impacted by perinatal TCDD exposure long after this exposure has ended, although the effects are subtle and likely to be uncovered only when microglia are actively participating in a pathological response. However, it is encouraging that microglia function can be recovered through repopulation of naïve microglia at a later point in life, suggesting additional therapeutic options for microglia-induced cortical dysfunction.

Supplementary Material

Refer to Web version on PubMed Central for supplementary material.

Acknowledgements:

We thank the Arnivan Ghosh Laboratory for the Sholl analysis ImageJ plug-in as well as the University of Rochester Flow Cytometry and Genomics Cores for facility usage.

Funding: This work was supported by the National Institutes of Health [grant numbers EY019277 (AKM), NS114480 (AKM), AA02711 (AKM), T32 ES007026 (RLL)]; the National Institute of Medical Sciences [grant number K12 GM106997 (SEL)]; the National Institute of Environmental Health Sciences [grant number P30ES001247 (AKM)]; and the National Institute of Child Health and Human Development [grant number P50HD103536–02 (AKM)]. These sponsors were not involved beyond providing study funding.

REFERENCES

Ames J, Warner M, Siracusa C, Signorini S, Brambilla P, Mocarelli P, Eskenazi B, 2019. Prenatal dioxin exposure and neuropsychological functioning in the Seveso Second Generation Health Study. Int J Hyg Environ Health 222, 425–433. [PubMed: 30638868]

Ayata P, Badimon A, Strasburger HJ, Duff MK, Montgomery SE, Loh YE, Ebert A, Pimenova AA, Ramirez BR, Chan AT, Sullivan JM, Purushothaman I, Scarpa JR, Goate AM, Busslinger M, Shen L, Losic B, Schaefer A, 2018. Epigenetic regulation of brain regionspecific microglia clearance activity. Nat Neurosci 21, 1049–1060. [PubMed: 30038282]

Barroso A, Mahler JV, Fonseca-Castro PH, Quintana FJ, 2021. The aryl hydrocarbon receptor and the gut-brain axis. Cell Mol Immunol 18, 259–268. [PubMed: 33408340]

Bennett ML, Bennett FC, Liddelow SA, Ajami B, Zamanian JL, Fernhoff NB, Mulinyawe SB, Bohlen CJ, Adil A, Tucker A, Weissman IL, Chang EF, Li G, Grant GA, Hayden Gephart MG, Barres BA, 2016. New tools for studying microglia in the mouse and human CNS. Proc Natl Acad Sci U S A 113, E1738–1746.

Bolger AM, Lohse M, Usadel B, 2014. Trimmomatic: a flexible trimmer for Illumina sequence data. Bioinformatics 30, 2114–2120. [PubMed: 24695404]

Bolton JL, Marinero S, Hassanzadeh T, Natesan D, Le D, Belliveau C, Mason SN, Auten RL, Bilbo SD, 2017. Gestational Exposure to Air Pollution Alters Cortical Volume, Microglial Morphology, and Microglia-Neuron Interactions in a Sex-Specific Manner. Front Synaptic Neurosci 9, 10. [PubMed: 28620294]

Boule LA, Burke CG, Jin GB, Lawrence BP, 2018. Aryl hydrocarbon receptor signaling modulates antiviral immune responses: ligand metabolism rather than chemical source is the stronger predictor of outcome. Sci Rep 8, 1826. [PubMed: 29379138]

Boule LA, Winans B, Lambert K, Vorderstrasse BA, Topham DJ, Pavelka MS Jr., Lawrence BP, 2015. Activation of the aryl hydrocarbon receptor during development enhances the pulmonary CD4+ T-cell response to viral infection. Am J Physiol Lung Cell Mol Physiol 309, L305–313. [PubMed: 26071552]

Bruttger J, Karram K, Wortge S, Regen T, Marini F, Hoppmann N, Klein M, Blank T, Yona S, Wolf Y, Mack M, Pinteaux E, Muller W, Zipp F, Binder H, Bopp T, Prinz M, Jung S, Waisman A, 2015. Genetic Cell Ablation Reveals Clusters of Local Self-Renewing Microglia in the Mammalian Central Nervous System. Immunity 43, 92–106. [PubMed: 26163371]

Cherry JD, Olschowka JA, O'Banion MK, 2015. Arginase 1+ microglia reduce Abeta plaque deposition during IL-1beta-dependent neuroinflammation. J Neuroinflammation 12, 203. [PubMed: 26538310]

Collins LL, Williamson MA, Thompson BD, Dever DP, Gasiewicz TA, Opanashuk LA, 2008. 2,3,7,8-Tetracholorodibenzo-p-dioxin exposure disrupts granule neuron precursor maturation in the developing mouse cerebellum. Toxicol Sci 103, 125–136. [PubMed: 18227101]

Davalos D, Grutzendler J, Yang G, Kim JV, Zuo Y, Jung S, Littman DR, Dustin ML, Gan WB, 2005. ATP mediates rapid microglial response to local brain injury in vivo. Nature Neuroscience 8, 752–758. [PubMed: 15895084]

Dever DP, Adham ZO, Thompson B, Genestine M, Cherry J, Olschowka JA, DiCicco-Bloom E, Opanashuk LA, 2016. Aryl hydrocarbon receptor deletion in cerebellar granule neuron precursors impairs neurogenesis. Dev Neurobiol 76, 533–550. [PubMed: 26243376]

Elmore MR, Najafi AR, Koike MA, Dagher NN, Spangenberg EE, Rice RA, Kitazawa M, Matusow B, Nguyen H, West BL, Green KN, 2014. Colony-stimulating factor 1 receptor signaling is necessary for microglia viability, unmasking a microglia progenitor cell in the adult brain. Neuron 82, 380–397. [PubMed: 24742461]

Elmore MRP, Hohsfield LA, Kramar EA, Soreq L, Lee RJ, Pham ST, Najafi AR, Spangenberg EE, Wood MA, West BL, Green KN, 2018. Replacement of microglia in the aged brain reverses cognitive, synaptic, and neuronal deficits in mice. Aging Cell 17, e12832.

Endo T, Kakeyama M, Uemura Y, Haijima A, Okuno H, Bito H, Tohyama C, 2012. Executive function deficits and social-behavioral abnormality in mice exposed to a low dose of dioxin in utero and via lactation. PLoS One 7, e50741.

Fallarino F, Romani L, Puccetti P, 2014. AhR: far more than an environmental sensor. Cell Cycle 13, 2645–2646. [PubMed: 25486345]

Fernandez-Salguero P, Pineau T, Hilbert DM, McPhail T, Lee SS, Kimura S, Nebert DW, Rudikoff S, Ward JM, Gonzalez FJ, 1995. Immune system impairment and hepatic fibrosis in mice lacking the dioxin-binding Ah receptor. Science 268, 722–726. [PubMed: 7732381]

Gasiewicz TA, Geiger LE, Rucci G, Neal RA, 1983. Distribution, excretion, and metabolism of 2,3,7,8-tetrachlorodibenzo-p-dioxin in C57BL/6J, DBA/2J, and B6D2F1/J mice. Drug Metab Dispos 11, 397–403. [PubMed: 6138222]

Grabert K, Michoel T, Karavolos MH, Clohisey S, Baillie JK, Stevens MP, Freeman TC, Summers KM, McColl BW, 2016. Microglial brain region-dependent diversity and selective regional sensitivities to aging. Nat Neurosci 19, 504–516. [PubMed: 26780511]

Gu YZ, Hogenesch JB, Bradfield CA, 2000. The PAS superfamily: sensors of environmental and developmental signals. Annu Rev Pharmacol Toxicol 40, 519–561. [PubMed: 10836146]

Guneykaya D, Ivanov A, Hernandez DP, Haage V, Wojtas B, Meyer N, Maricos M, Jordan P, Buonfiglioli A, Gielniewski B, Ochocka N, Comert C, Friedrich C, Artiles LS, Kaminska B, Mertins P, Beule D, Kettenmann H, Wolf SA, 2018. Transcriptional and Translational Differences of Microglia from Male and Female Brains. Cell Rep 24, 2773–2783 e2776.

Haijima A, Endo T, Zhang Y, Miyazaki W, Kakeyama M, Tohyama C, 2010. In utero and lactational exposure to low doses of chlorinated and brominated dioxins induces deficits in the fear memory of male mice. Neurotoxicology 31, 385–390. [PubMed: 20398696]

Hanamsagar R, Alter MD, Block CS, Sullivan H, Bolton JL, Bilbo SD, 2017. Generation of a microglial developmental index in mice and in humans reveals a sex difference in maturation and immune reactivity. Glia 65, 1504–1520. [PubMed: 28618077]

Hojo R, Stern S, Zareba G, Markowski VP, Cox C, Kost JT, Weiss B, 2002. Sexually dimorphic behavioral responses to prenatal dioxin exposure. Environ Health Perspect 110, 247–254. [PubMed: 11882475]

Ikeda M, Mitsui T, Setani K, Tamura M, Kakeyama M, Sone H, Tohyama C, Tomita T, 2005. In utero and lactational exposure to 2,3,7,8-tetrachlorodibenzo-p-dioxin in rats disrupts brain sexual differentiation. Toxicol Appl Pharmacol 205, 98–105. [PubMed: 15885269]

Jung S, Aliberti J, Graemmel P, Sunshine MJ, Kreutzberg GW, Sher A, Littman DR, 2000. Analysis of fractalkine receptor CX(3)CR1 function by targeted deletion and green fluorescent protein reporter gene insertion. Mol Cell Biol 20, 4106–4114. [PubMed: 10805752]

Juricek L, Carcaud J, Pelhaitre A, Riday TT, Chevallier A, Lanzini J, Auzeil N, Laprevote O, Dumont F, Jacques S, Letourneur F, Massaad C, Agulhon C, Barouki R, Beraneck M, Coumoul X, 2017. AhR-deficiency as a cause of demyelinating disease and inflammation. Sci Rep 7, 9794. [PubMed: 28851966]

Kakeyama M, Endo T, Zhang Y, Miyazaki W, Tohyama C, 2014. Disruption of paired-associate learning in rat offspring perinatally exposed to dioxins. Arch Toxicol 88, 789–798. [PubMed: 24292196]

Kerkvliet NI, 1995. Immunological effects of chlorinated dibenzo-p-dioxins. Environ Health Perspect 103 Suppl 9, 47–53.

Kettenmann H, Hanisch UK, Noda M, Verkhratsky A, 2011. Physiology of microglia. Physiol Rev 91, 461–553. [PubMed: 21527731]

Kimura E, Kubo KI, Endo T, Ling W, Nakajima K, Kakeyama M, Tohyama C, 2017a. Impaired dendritic growth and positioning of cortical pyramidal neurons by activation of aryl hydrocarbon receptor signaling in the developing mouse. PLoS One 12, e0183497.

Kimura E, Kubo KI, Endo T, Nakajima K, Kakeyama M, Tohyama C, 2017b. Excessive activation of AhR signaling disrupts neuronal migration in the hippocampal CA1 region in the developing mouse. J Toxicol Sci 42, 25–30. [PubMed: 28070106]

Kimura E, Tohyama C, 2017. Embryonic and Postnatal Expression of Aryl Hydrocarbon Receptor mRNA in Mouse Brain. Front Neuroanat 11, 4. [PubMed: 28223923]

Kolluri SK, Weiss C, Koff A, Gottlicher M, 1999. p27(Kip1) induction and inhibition of proliferation by the intracellular Ah receptor in developing thymus and hepatoma cells. Genes Dev 13, 1742–1753. [PubMed: 10398686]

Latchney SE, Hein AM, O'Banion MK, DiCicco-Bloom E, Opanashuk LA, 2013. Deletion or activation of the aryl hydrocarbon receptor alters adult hippocampal neurogenesis and contextual fear memory. J Neurochem 125, 430–445. [PubMed: 23240617]

Latchney SE, Majewska AK, 2021. Persistent organic pollutants at the synapse: Shared phenotypes and converging mechanisms of developmental neurotoxicity. Dev Neurobiol 81, 623652.

Law CW, Chen Y, Shi W, Smyth GK, 2014. voom: Precision weights unlock linear model analysis tools for RNA-seq read counts. Genome Biol 15, R29. [PubMed: 24485249]

Lee YH, Lin CH, Hsu PC, Sun YY, Huang YJ, Zhuo JH, Wang CY, Gan YL, Hung CC, Kuan CY, Shie FS, 2015. Aryl hydrocarbon receptor mediates both proinflammatory and antiinflammatory effects in lipopolysaccharide-activated microglia. Glia 63, 1138–1154. [PubMed: 25690886]

Lenz KM, Nugent BM, Haliyur R, McCarthy MM, 2013. Microglia are essential to masculinization of brain and behavior. J Neurosci 33, 2761–2772. [PubMed: 23407936]

Li Y, Chen G, Zhao J, Nie X, Wan C, Liu J, Duan Z, Xu G, 2013. 2,3,7,8-Tetrachlorodibenzo-pdioxin (TCDD) induces microglial nitric oxide production and subsequent rat primary cortical neuron apoptosis through p38/JNK MAPK pathway. Toxicology 312, 132–141. [PubMed: 23969120]

Liao X, Yang J, Wang H, Li Y, 2020. Microglia mediated neuroinflammation in autism spectrum disorder. J Psychiatr Res 130, 167–176. [PubMed: 32823050]

Livak KJ, Schmittgen TD, 2001. Analysis of relative gene expression data using real-time quantitative PCR and the 2(-Delta Delta C(T)) Method. Methods 25, 402–408. [PubMed: 11846609]

Lowery RL, Latchney SE, Peer RP, Lamantia CE, Opanashuk L, McCall M, Majewska AK, 2021. Acute 2,3,7,8-Tetrachlorodibenzo-p-dioxin exposure in adult mice does not alter the morphology or inflammatory response of cortical microglia. Neurosci Lett 742, 135516.

Mandal PK, 2005. Dioxin: a review of its environmental effects and its aryl hydrocarbon receptor biology. J Comp Physiol B 175, 221–230. [PubMed: 15900503]

Markowski VP, Cox C, Preston R, Weiss B, 2002. Impaired cued delayed alternation behavior in adult rat offspring following exposure to 2,3,7,8-tetrachlorodibenzo-p-dioxin on gestation day 15. Neurotoxicol Teratol 24, 209–218. [PubMed: 11943508]

Marshall NB, Kerkvliet NI, 2010. Dioxin and immune regulation: emerging role of aryl hydrocarbon receptor in the generation of regulatory T cells. Ann N Y Acad Sci 1183, 25–37. [PubMed: 20146706]

Masuda T, Sankowski R, Staszewski O, Prinz M, 2020. Microglia Heterogeneity in the Single-Cell Era. Cell Rep 30, 1271–1281. [PubMed: 32023447]

Mendes MS, Le L, Atlas J, Brehm Z, Ladron-de-Guevara A, Matei E, Lamantia C, McCall MN, Majewska AK, 2021. The role of P2Y12 in the kinetics of microglial self-renewal and maturation in the adult visual cortex in vivo. Elife 10.

Mendes MS, Majewska AK, 2021. An overview of microglia ontogeny and maturation in the homeostatic and pathological brain. Eur J Neurosci 53, 3525–3547. [PubMed: 33835613]

Mitsuhashi T, Yonemoto J, Sone H, Kosuge Y, Kosaki K, Takahashi T, 2010. In utero exposure to dioxin causes neocortical dysgenesis through the actions of p27Kip1. Proc Natl Acad Sci U S A 107, 16331–16335.

Nguyen MN, Nishijo M, Nguyen AT, Bor A, Nakamura T, Hori E, Nakagawa H, Ono T, Nishijo H, 2013. Effects of maternal exposure to 2,3,7,8-tetrachlorodibenzo-p-dioxin on parvalbumin- and calbindin-immunoreactive neurons in the limbic system and superior colliculus in rat offspring. Toxicology 314, 125–134. [PubMed: 24060430]

Nimmerjahn A, Kirchhoff F, Helmchen F, 2005. Resting microglial cells are highly dynamic surveillants of brain parenchyma in vivo. Science 308, 1314–1318. [PubMed: 15831717]

Nishijo M, Tai PT, Nakagawa H, Maruzeni S, Anh NT, Luong HV, Anh TH, Honda R, Morikawa Y, Kido T, Nishijo H, 2012. Impact of perinatal dioxin exposure on infant growth: a cross-sectional and longitudinal studies in dioxin-contaminated areas in Vietnam. PLoS One 7, e40273.

Norden DM, Muccigrosso MM, Godbout JP, 2015. Microglial priming and enhanced reactivity to secondary insult in aging, and traumatic CNS injury, and neurodegenerative disease. Neuropharmacology 96, 29–41. [PubMed: 25445485]

O'Neil SM, Witcher KG, McKim DB, Godbout JP, 2018. Forced turnover of aged microglia induces an intermediate phenotype but does not rebalance CNS environmental cues driving priming to immune challenge. Acta Neuropathol Commun 6, 129. [PubMed: 30477578]

Perry VH, Holmes C, 2014. Microglial priming in neurodegenerative disease. Nat Rev Neurol 10, 217–224. [PubMed: 24638131]

Quintana FJ, Basso AS, Iglesias AH, Korn T, Farez MF, Bettelli E, Caccamo M, Oukka M, Weiner HL, 2008. Control of T(reg) and T(H)17 cell differentiation by the aryl hydrocarbon receptor. Nature 453, 65–71. [PubMed: 18362915]

Rice RA, Pham J, Lee RJ, Najafi AR, West BL, Green KN, 2017. Microglial repopulation resolves inflammation and promotes brain recovery after injury. Glia 65, 931–944. [PubMed: 28251674]

Rice RA, Spangenberg EE, Yamate-Morgan H, Lee RJ, Arora RP, Hernandez MX, Tenner AJ, West BL, Green KN, 2015. Elimination of Microglia Improves Functional Outcomes Following Extensive Neuronal Loss in the Hippocampus. J Neurosci 35, 9977–9989. [PubMed: 26156998]

Rothhammer V, Borucki DM, Tjon EC, Takenaka MC, Chao CC, Ardura-Fabregat A, de Lima KA, Gutierrez-Vazquez C, Hewson P, Staszewski O, Blain M, Healy L, Neziraj T, Borio M, Wheeler M, Dragin LL, Laplaud DA, Antel J, Alvarez JI, Prinz M, Quintana FJ, 2018. Microglial control of astrocytes in response to microbial metabolites. Nature 557, 724–728. [PubMed: 29769726]

Schwarz JM, Sholar PW, Bilbo SD, 2012. Sex differences in microglial colonization of the developing rat brain. J Neurochem 120, 948–963. [PubMed: 22182318]

Shahidehpour RK, Higdon RE, Crawford NG, Neltner JH, Ighodaro ET, Patel E, Price D, Nelson PT, Bachstetter AD, 2021. Dystrophic microglia are associated with neurodegenerative disease and not healthy aging in the human brain. Neurobiol Aging 99, 19–27. [PubMed: 33422891]

Sierra A, Paolicelli RC, Kettenmann H, 2019. Cien Anos de Microglia: Milestones in a Century of Microglial Research. Trends Neurosci 42, 778–792. [PubMed: 31635851]

Sipe GO, Lowery RL, Tremblay ME, Kelly EA, Lamantia CE, Majewska AK, 2016. Microglial P2Y12 is necessary for synaptic plasticity in mouse visual cortex. Nat Commun 7, 10905.

Stevens EA, Mezrich JD, Bradfield CA, 2009. The aryl hydrocarbon receptor: a perspective on potential roles in the immune system. Immunology 127, 299–311. [PubMed: 19538249]

Stowell RD, Sipe GO, Dawes RP, Batchelor HN, Lordy KA, Whitelaw BS, Stoessel MB, Bidlack JM, Brown E, Sur M, Majewska AK, 2019. Noradrenergic signaling in the wakeful state inhibits microglial surveillance and synaptic plasticity in the mouse visual cortex. Nat Neurosci 22, 1782–1792. [PubMed: 31636451]

Tai PT, Nishijo M, Anh NT, Maruzeni S, Nakagawa H, Van Luong H, Anh TH, Honda R, Kido T, Nishijo H, 2013. Dioxin exposure in breast milk and infant neurodevelopment in Vietnam. Occup Environ Med 70, 656–662. [PubMed: 23390198]

Thion MS, Low D, Silvin A, Chen J, Grisel P, Schulte-Schrepping J, Blecher R, Ulas T, Squarzoni P, Hoeffel G, Coulpier F, Siopi E, David FS, Scholz C, Shihui F, Lum J, Amoyo AA, Larbi

A, Poidinger M, Buttgereit A, Lledo PM, Greter M, Chan JKY, Amit I, Beyer M, Schultze JL, Schlitzer A, Pettersson S, Ginhoux F, Garel S, 2018. Microbiome Influences Prenatal and Adult Microglia in a Sex-Specific Manner. Cell 172, 500–516 e516.

Vorderstrasse BA, Cundiff JA, Lawrence BP, 2004. Developmental exposure to the potent aryl hydrocarbon receptor agonist 2,3,7,8-tetrachlorodibenzo-p-dioxin Impairs the cell-mediated immune response to infection with influenza a virus, but enhances elements of innate immunity. J Immunotoxicol 1, 103–112. [PubMed: 18958643]

Vorderstrasse BA, Cundiff JA, Lawrence BP, 2006. A dose-response study of the effects of prenatal and lactational exposure to TCDD on the immune response to influenza a virus. J Toxicol Environ Health A 69, 445–463. [PubMed: 16574621]

Vorderstrasse BA, Kerkvliet NI, 2001. 2,3,7,8-Tetrachlorodibenzo-p-dioxin affects the number and function of murine splenic dendritic cells and their expression of accessory molecules. Toxicol Appl Pharmacol 171, 117–125. [PubMed: 11222087]

Vorderstrasse BA, Steppan LB, Silverstone AE, Kerkvliet NI, 2001. Aryl hydrocarbon receptordeficient mice generate normal immune responses to model antigens and are resistant to TCDDinduced immune suppression. Toxicol Appl Pharmacol 171, 157–164. [PubMed: 11243915]

Vos JG, De Heer C, Van Loveren H, 1997. Immunotoxic effects of TCDD and toxic equivalency factors. Teratog Carcinog Mutagen 17, 275–284. [PubMed: 9508737]

Wei GZ, Martin KA, Xing PY, Agrawal R, Whiley L, Wood TK, Hejndorf S, Ng YZ, Low JZY, Rossant J, Nechanitzky R, Holmes E, Nicholson JK, Tan EK, Matthews PM, Pettersson S, 2021. Tryptophan-metabolizing gut microbes regulate adult neurogenesis via the aryl hydrocarbon receptor. Proc Natl Acad Sci U S A 118.

Wheeler JL, Martin KC, Resseguie E, Lawrence BP, 2014. Differential consequences of two distinct AhR ligands on innate and adaptive immune responses to influenza A virus. Toxicol Sci 137, 324–334. [PubMed: 24194396]

Williamson MA, Gasiewicz TA, Opanashuk LA, 2005. Aryl hydrocarbon receptor expression and activity in cerebellar granule neuroblasts: implications for development and dioxin neurotoxicity. Toxicol Sci 83, 340–348. [PubMed: 15537747]

Winans B, Nagari A, Chae M, Post CM, Ko CI, Puga A, Kraus WL, Lawrence BP, 2015. Linking the aryl hydrocarbon receptor with altered DNA methylation patterns and developmentally induced aberrant antiviral CD8+ T cell responses. J Immunol 194, 4446–4457. [PubMed: 25810390]

Wong EL, Lutz NM, Hogan VA, Lamantia CE, McMurray HR, Myers JR, Ashton JM, Majewska AK, 2018. Developmental alcohol exposure impairs synaptic plasticity without overtly altering microglial function in mouse visual cortex. Brain Behav Immun 67, 257–278. [PubMed: 28918081]

World Health Organization, 2016. Dioxins and their effects on human health.

Wu D, Lim E, Vaillant F, Asselin-Labat ML, Visvader JE, Smyth GK, 2010. ROAST: rotation gene set tests for complex microarray experiments. Bioinformatics 26, 2176–2182. [PubMed: 20610611]

Xu G, Li Y, Yoshimoto K, Chen G, Wan C, Iwata T, Mizusawa N, Duan Z, Liu J, Jiang J, 2013. 2,3,7,8-Tetrachlorodibenzo-p-dioxin-induced inflammatory activation is mediated by intracellular free calcium in microglial cells. Toxicology 308, 158–167. [PubMed: 23583884]

Xu G, Liu J, Yoshimoto K, Chen G, Iwata T, Mizusawa N, Duan Z, Wan C, Jiang J, 2014. 2,3,7,8-tetrachlorodibenzo-p-dioxin (TCDD) induces expression of p27(kip(1)) and FoxO3a in female rat cerebral cortex and PC12 cells. Toxicol Lett 226, 294–302. [PubMed: 24594276]

Zhan L, Fan L, Kodama L, Sohn PD, Wong MY, Mousa GA, Zhou Y, Li Y, Gan L, 2020. A MAC2-positive progenitor-like microglial population is resistant to CSF1R inhibition in adult mouse brain. Elife 9.

Zhang Y, Chen K, Sloan SA, Bennett ML, Scholze AR, O'Keeffe S, Phatnani HP, Guarnieri P, Caneda C, Ruderisch N, Deng S, Liddelow SA, Zhang C, Daneman R, Maniatis T, Barres BA, Wu JQ, 2014. An RNA-sequencing transcriptome and splicing database of glia, neurons, and vascular cells of the cerebral cortex. J Neurosci 34, 11929–11947.

HIGHLIGHTS

- Baseline microglia function reamains intact after perinatal TCDD exposure.
- Microglial response to pathological stimuli is altered by perinatal TCDD exposure.
- Functional changes after perinatal TCDD exposure can be rectified by microglial repopulation.

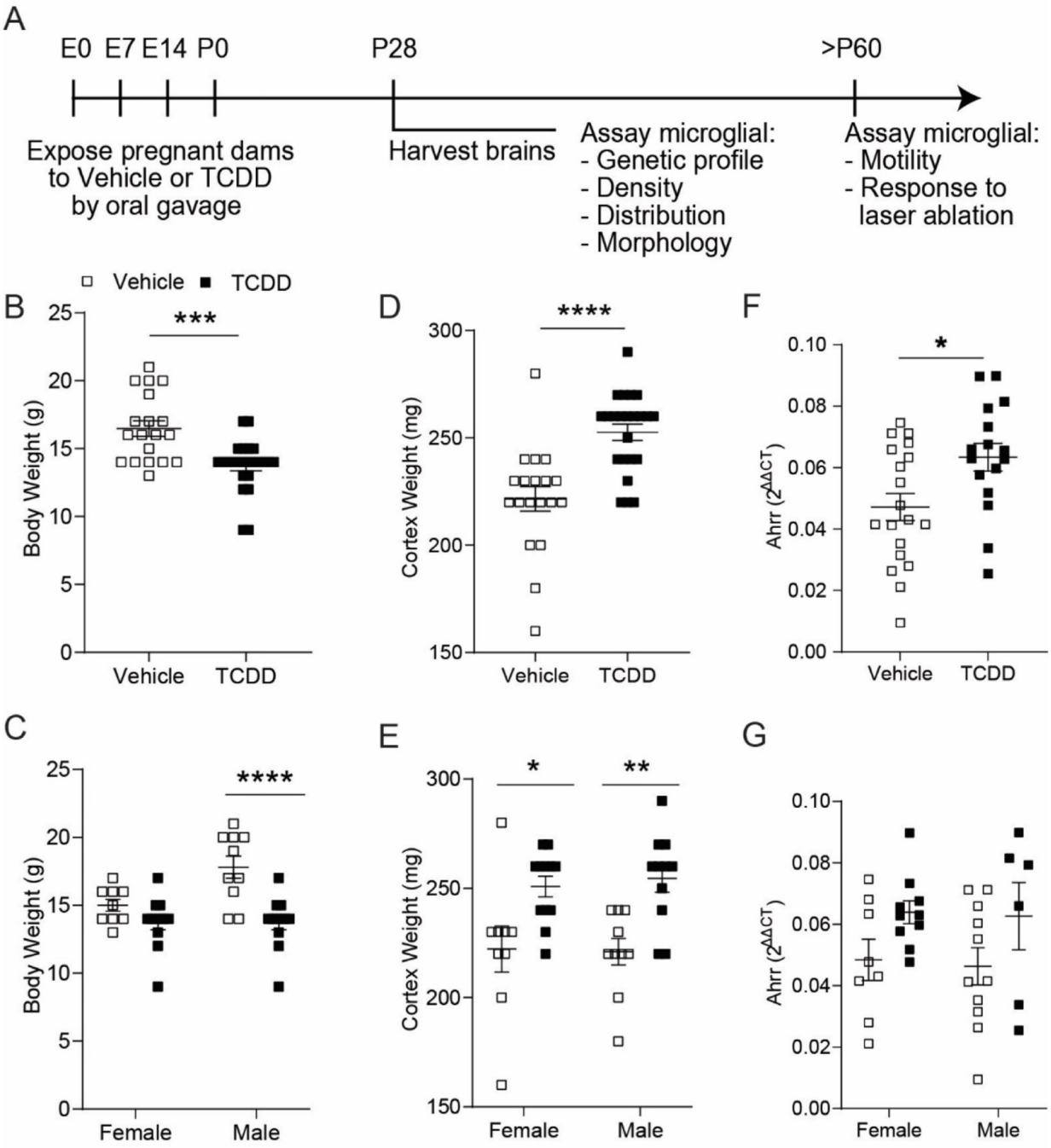

Figure 1.

(A) Timeline of perinatal TCDD exposure. **(B)** C57Bl/6J mice exposed to TCDD weighed significantly less than vehicle-exposed mice at P28 (n = 19–24 animals per group; unpaired t-test, P = 0.0002) **(C)** This weight loss was evident only in TCDD-exposed males (n = 9–12 animals per group; two-way ANOVA, interaction: P = 0.0274; sex: P = 0.0274; exposure: P < 0.0001; Bonferroni post-hoc, females: P = 0.3236; males: P < 0.0001). **(D)** P28 TCDD-exposed cortices weighed significantly more compared to vehicle-exposed cortices (n = 19–23 animals per group; unpaired t-test, P < 0.0001). **(E)** This weight gain was evident in

both TCDD-exposed males and females (n = 9–12 animals per group; two-way ANOVA, interaction: $P = 0.7214$; sex: $P = 0.8571$, exposure: $P < 0.0001$; Bonferroni post-hoc, females: $P = 0.0114$; males: $P = 0.0026$). **(F, G)** Ahrr expression is significantly increased following perinatal TCDD exposure, with no significant sex difference (n=16–19 animals per group; unpaired t-test, $P < 0.0150$). *$P < 0.05$, **$P < 0.01$, ***$P < 0.001$, ****$P < 0.0001$ vs. vehicle. Graphs show individual data points and mean ± SEM.

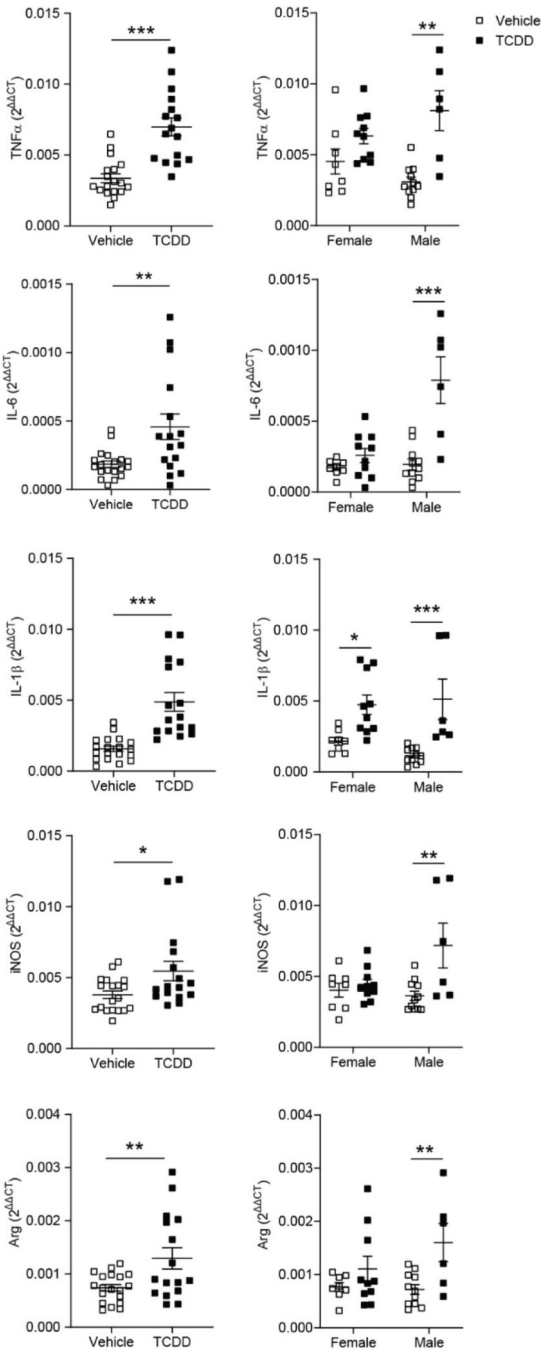

Figure 2.

RT-qPCR analysis of **(A)** *Tnf*-α, **(B)** *IL-6,* **(C)** *Il-1β,* **(D)** *iNos,* **(E)** and *Arginase* mRNA expression from P28 cortices of C57Bl/6J mice exposed to vehicle or TCDD during gestation and lactation. mRNA expression was normalized to the expression of three reference genes, *Gapdh*, *β-Actin*, and Eif2b1. For all genes, TCDD-exposed mice had significantly increased expression compared to their vehicle-exposed equivalents (n = 16–19 animals per group). When analyzed by sex, only TCDD-exposed male mice exhibited a significant increase in gene expression for all cytokines tested (n = 6–11 animals per group).

$^{*}P < 0.05$, $^{**}P < 0.01$, $^{***}P < 0.001$ vs. vehicle. Graphs show individual data points and mean ± SEM.

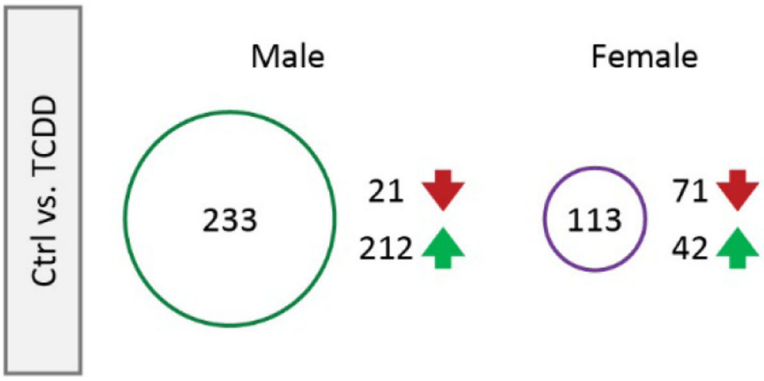

Figure 3.

RT-qPCR analysis of microglia following gestational TCDD exposure. 346 genes had a logfc greater than or equal to 1.5. The number of affected genes and the direction of change differed between males and females.

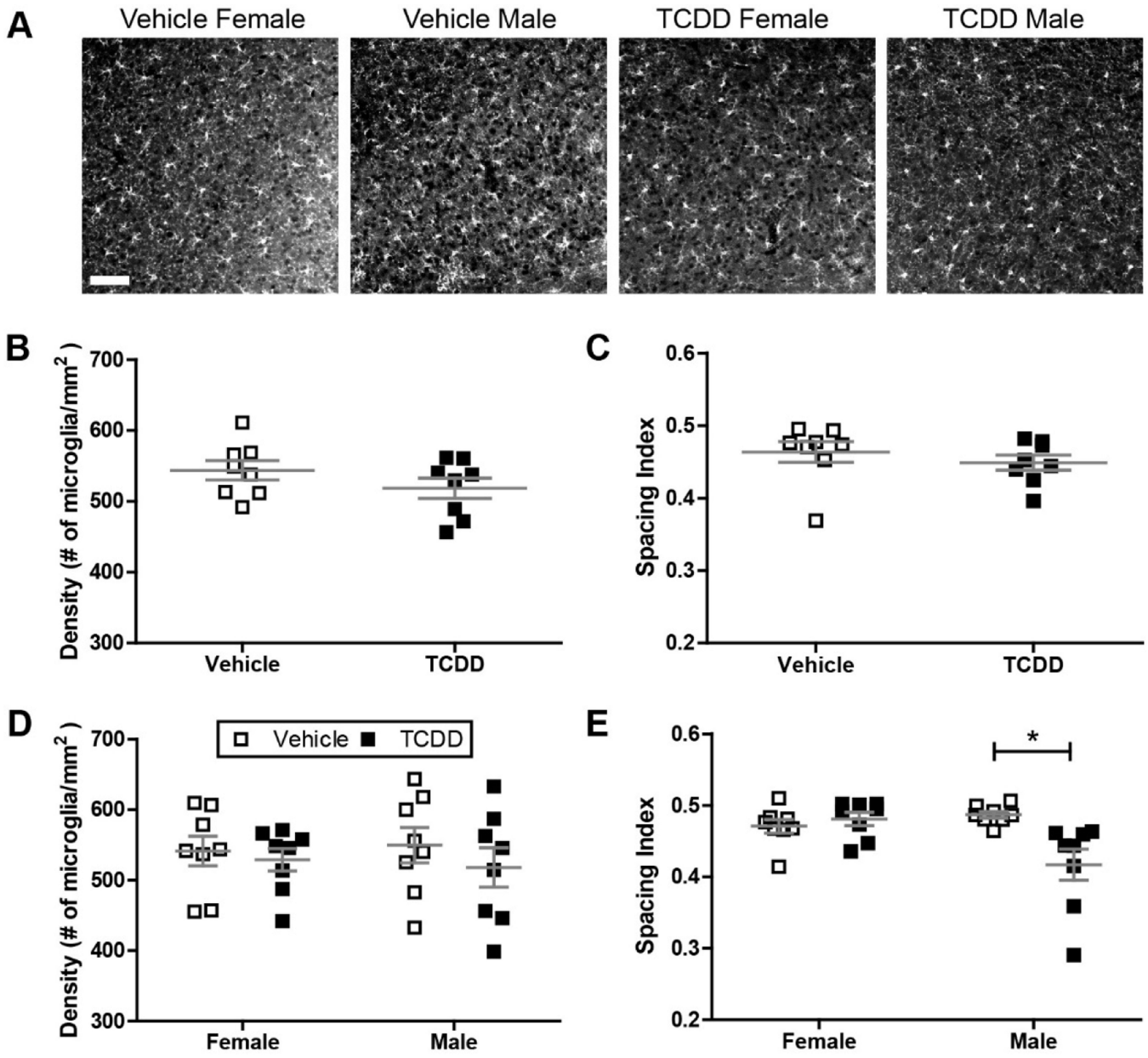

Figure 4.

(A) Representative images showing Iba1+ microglia in binocular primary visual cortex of male and female C57Bl/6J mice at P28 after exposure to vehicle or TCDD during gestation and lactation. Scale bar = 50μm. **(B,C)** There is no significant difference in microglial density or distribution throughout binocular visual cortex across treatment groups. **(D,E)** There is no sex-specific effect on microglia density, but TCDD induces a small change in microglia distribution in male mice (n = 8 litters per condition, two-way ANOVA, interaction: P = 0.0047, sex: P = 0.0768, exposure: P = 0.0291; Bonferroni post-hoc: P = 0.0034). *P < 0.01. Data points represent litter averages and graphs show mean ± SEM.

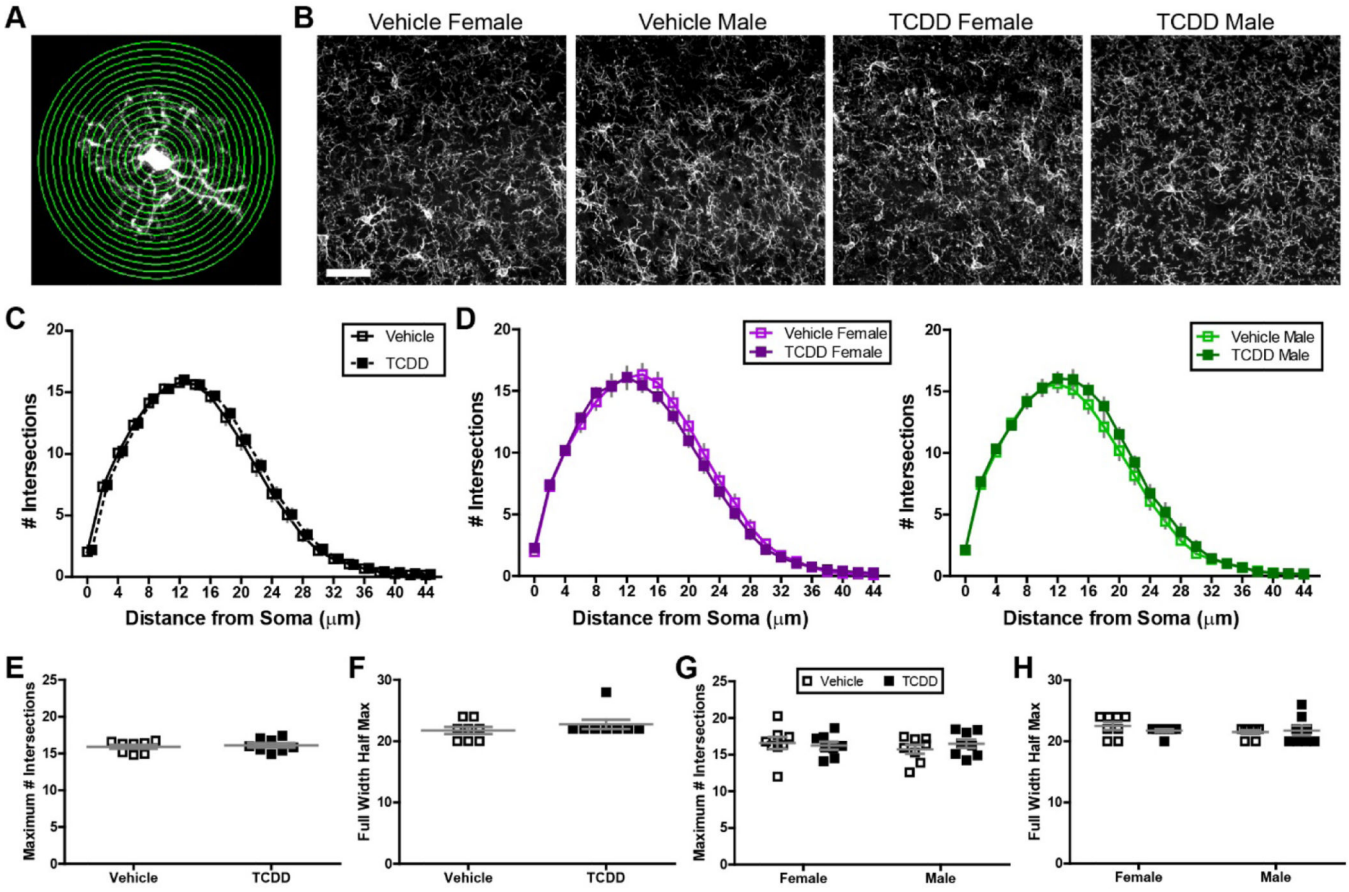

Figure 5.

(A) Image representing Sholl analysis on Iba1+ microglia. Concentric circles are drawn at varying distance from the soma and intersections between these circles and the microglial arbor are quantified. **(B)** Representative images of Iba1+ microglia in binocular primary visual cortex of male and female C57Bl/6J mice at P28 after exposure to vehicle or TCDD. Scale bar = 20μm. Microglial process arbor complexity is similar across treatment groups in the combined data set **(C)** and in males and females analyzed separately **(D). (E-F)** There is no significant difference in the height (maximum number of intersections, E) or width (full width half max, F) of the Sholl distribution. **(G-H)** There is no sex-specific effect on microglial process arbor complexity across treatment groups. Data points represent litter averages and graphs show mean ± SEM.

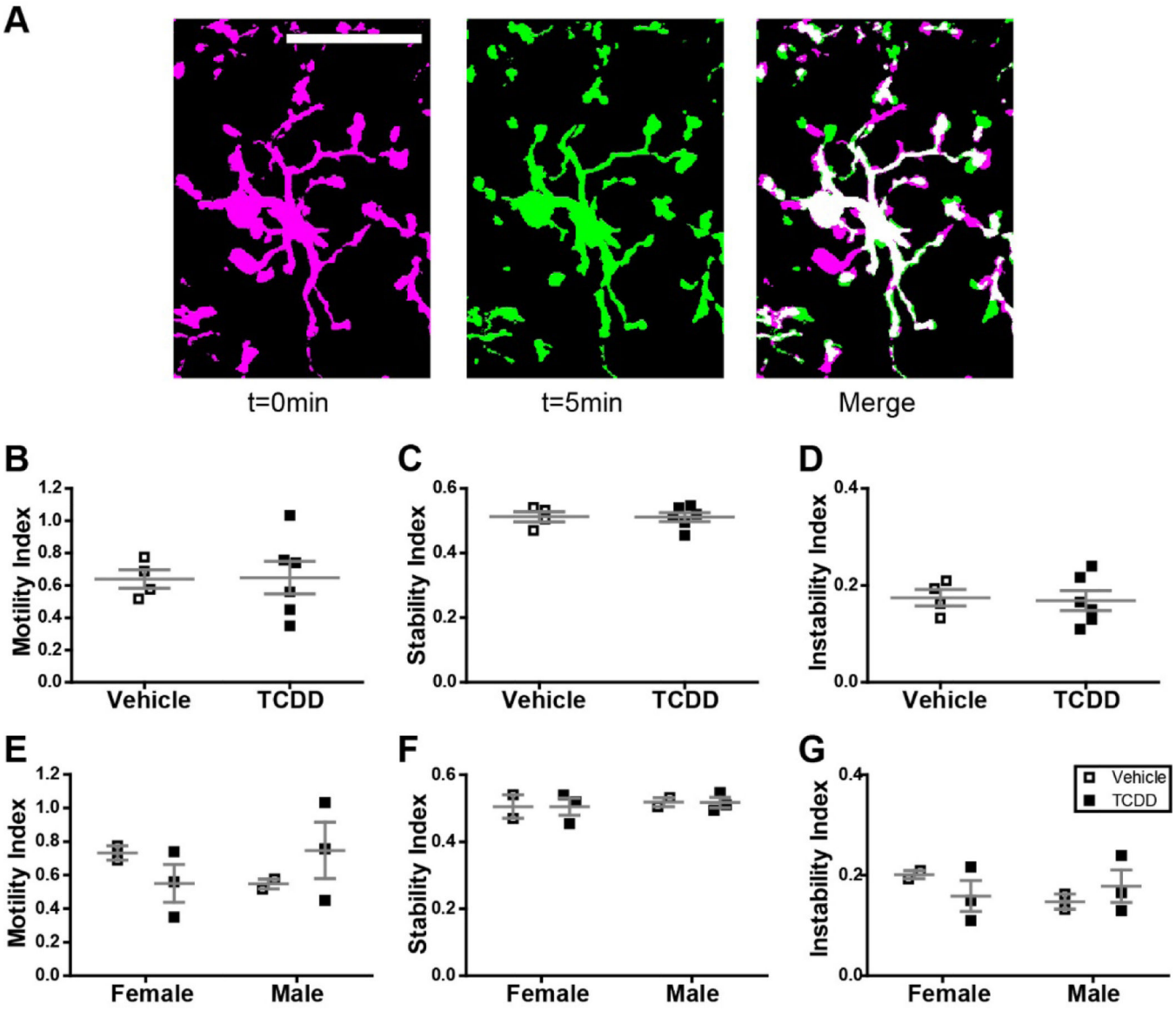

Figure 6.

(**A)** Schematic representation of motility analysis. Images of *Cx3cr1*$^{G/+}$ mice developmentally exposed to either vehicle or TCDD were collected every 5 minutes for 1 hour. To assay process motility, each microglia was analyzed individually across all time points. Time point t = 0 minutes was pseudocolored magenta, time point t = 5 minutes was pseudocolored green, and the two time points were overlaid to generate the merged image. In this image, magenta pixels represent processes which have retracted, green pixels represent pixels which have extended, and white pixels represent processes which remained stable. This analysis was performed for all adjacent pairs of time points. Scale bar = 20μm. **(B-G**) There is no significant difference in microglia process motility, stability, or instability across treatment groups in the combined data set or when analyzed for effect of sex. Graphs show individual data points and mean ± SEM.

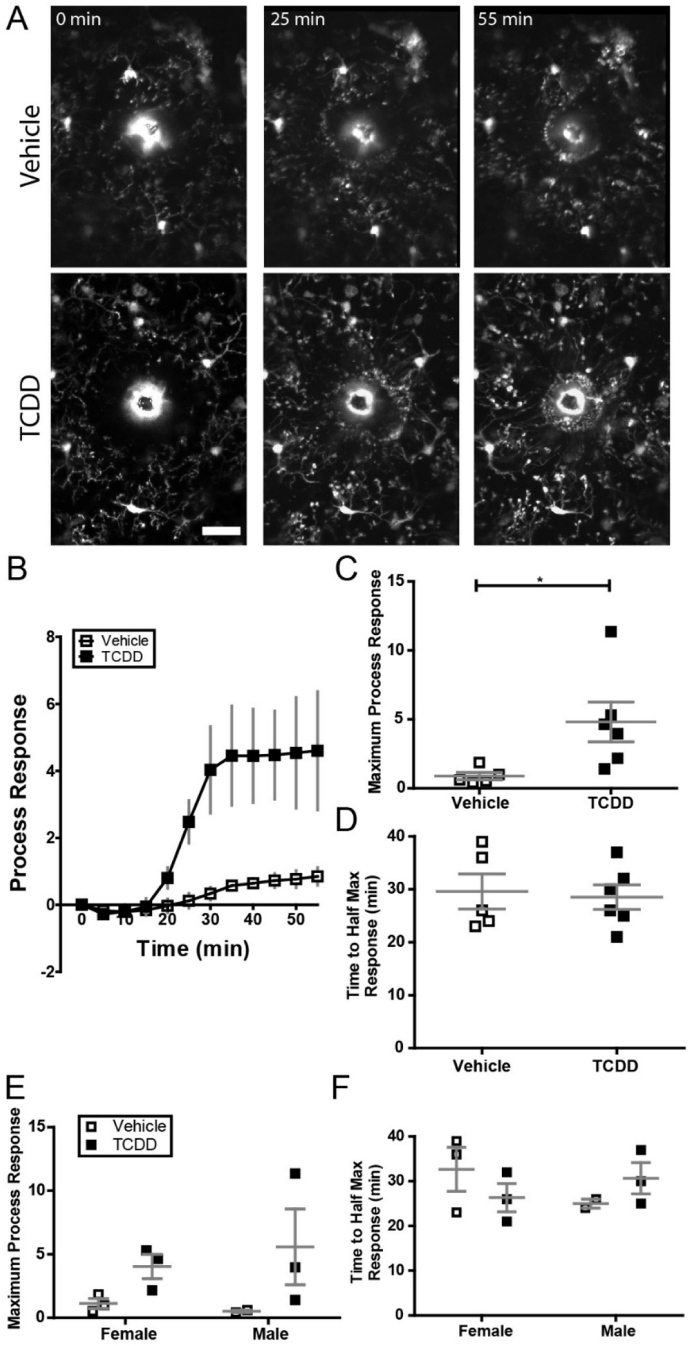

Figure 7.

(A) Representative images of microglial response to focal laser ablation insult over the course of 1 hour in binocular primary visual cortex of *Cx3Cr1*$^{G/+}$ mice exposed to either vehicle or TCDD during gestation and lactation. Notice the microglial processes accumulating at the autofluorescent injury core over the course of the experiment. Scale bar = 20μm. **(B)** Time course of microglial process response to focal laser ablation insult in mice exposed to vehicle or TCDD. **(C)** Mice exposed to TCDD exhibit a significantly higher microglial process response to focal laser ablation injury than vehicle-exposed mice (*n* =

5 animals per group; unpaired t-test, $P = 0.0384$). **(D)** There is no significant difference in speed of process response across groups. $*P < 0.05$; Graphs show individual data points and mean ± SEM.

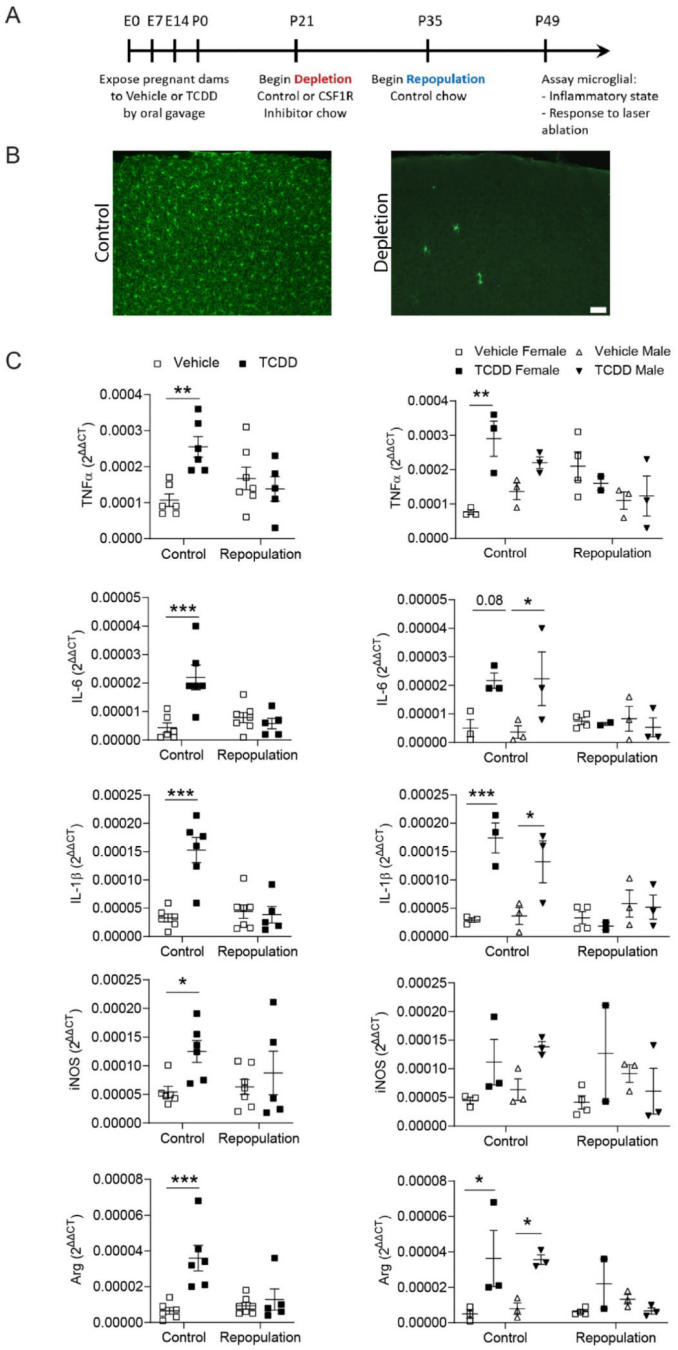

Figure 8.

(A) Timeline of microglial repopulation. **(B)** Representative images of control microglia and microglial depletion following treatment with CSF1R inhibitor. Scale bar = 50μm. **(C)** RTqPCR analysis of *Tnf*-α*, IL-6, Il-1β, iNos,* and *Arginase* mRNA expression from P49 cortices of C57Bl/6J mice exposed to vehicle or TCDD during gestation and lactation and later receiving control chow or chow containing a CSF1R inhibitor. TCDD-exposed mice had significantly increased expression compared to their vehicle-exposed equivalents only in the control chow condition. Following microglial repopulation, expression levels did

not significantly different from vehicle-exposure (n = 5–7 animals per condition). While the small sample size precluded rigorous analysis, when analyzed by sex, no significant differences were found between vehicle- and TCDD-exposed mice following microglial repopulation (n = 2–3 animals per group). mRNA expression was normalized to the expression of three reference genes, *Gapdh, β-Actin*, and Eif2b1. Graphs show individual data points and mean ± SEM.

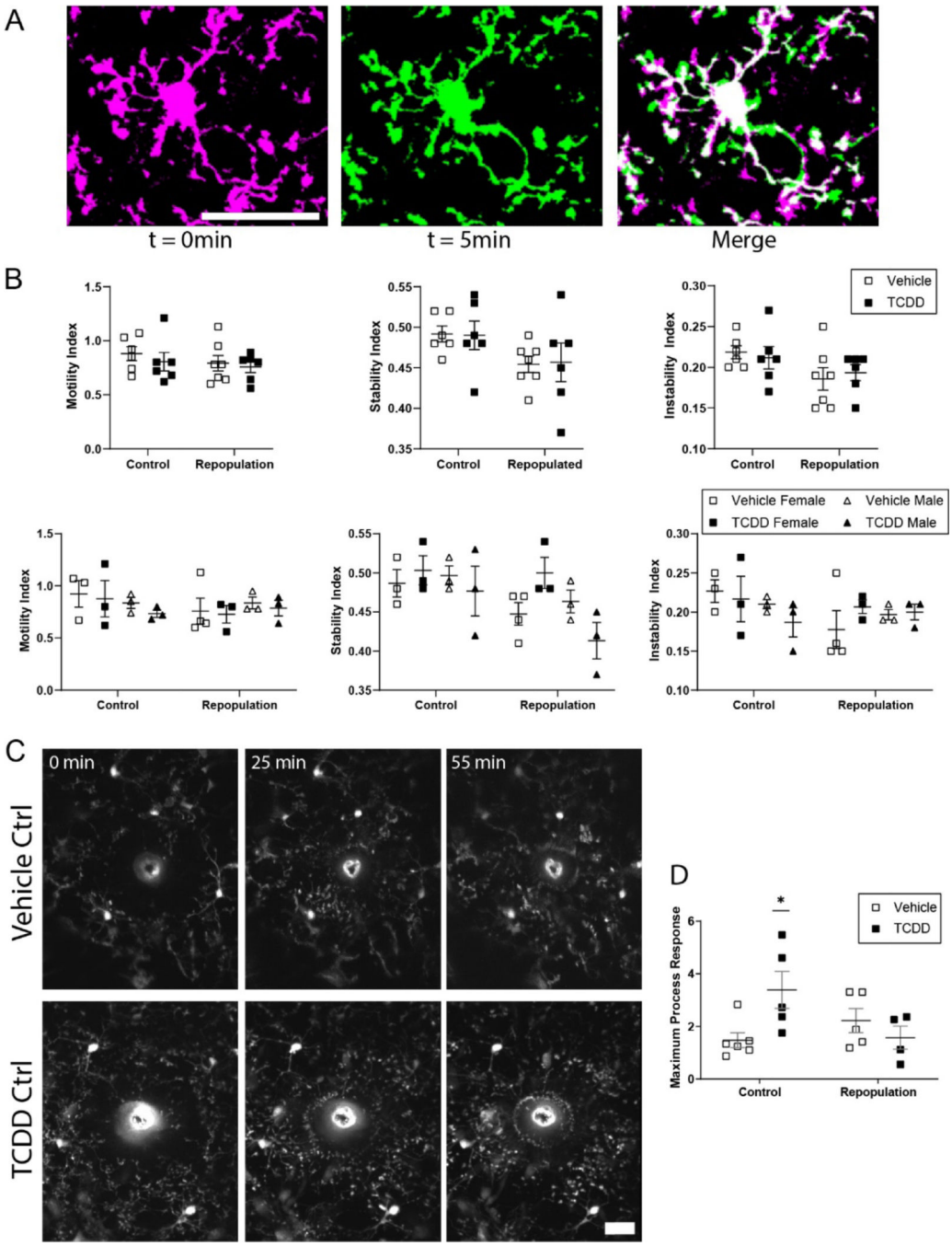

Figure 9.

(A) Representative images of microglial process motility across a 5-minute period. Scale bar = 20μm. **(B)** There is no significant difference in microglia process motility, stability, or instability across treatment groups regardless of repopulation state, either in the combined data set or when analyzed for effect of sex. **(C)** Representative images of microglial process response to a laser-induced focal tissue injury over a 1-hour period. Scale bar = 20μm. **(D)** Mice exposed to TCDD exhibit a significantly higher microglial process response to focal laser ablation injury than vehicle-exposed mice, while this response

has been normalized following microglial repopulation (n = 4–6 animals per group; two-way ANOVA, interaction: P = 0.0166, exposure: P = 0.3139, repopulation: P = 0.4096; Bonferroni post-hoc test, P = 0.0232.) Graphs show individual data points and mean ± SEM.

Table 1.

List of primer sequences used for QPCR.

Gene	Forward	Reverse
β-actin	5′-CCTCTATGCCAACACAGTGC-3′	5′-CCTGCTTGCTGATCCACATC-3′
Gapdh	5′-CAACTCCCACTCTTCCACCT-3′	5′-GAGTTGGGATAGGGCCTCTC-3′
Eif2b1	5’-CAGGAGGACGTCCCAGATAA-3’	5’-AGCGACTCGGCTCATAGGTA-3’
Il-1β	5′-CAACAGAGAGCAACCAGAGC-3′	5′-TCATCTTTTGGGGTCCGTCA-3′
Tnf-α	5’-GACCCCTTTACTCTGACCCC-3’	5’-AGGCTCCAGTGAATTCGGAA-3’
Il-6	5′-TACCACTCCCAACAGACCTG-3′	5′-ACTCCAGAAGACCAGAGGAA-3′
iNos	5’-TGACGCTCGGAACTGTAGCAC-3’	5’-TGATGGCCGACCTGATGTT-3’
Arginase	5’-ACAAGACAGGGCTCCTTTCAG-3’	5’-GGCTTATGGTTACCCTCCCG-3’
Ahrr	5′-GAGGCCAGGTCCCAGAGATGAGAGA-3’	5′-GGGGCGCAGAAGATCGGGCG-3′

Table 2

Statistical results from cytokine analyses presented in Figs. 2 and 8.

Cytokine Statistics												
Fig. 2	**t-test**		**Two-way ANOVA**						**Post-hoc**			
			Interaction		**Sex**		**TCDD**		**Female**		**Male**	
	P value	**Test Stat**	**P value**	**Test Stat**	**P value**	**Test Stat**	**P value**	**Test Stat**	**P value**	**Test Stat**	**P value**	**Test Stat**
Tnf-α	$p < 0.0001$	$t(32) = 5.294$	$p = 0.0381$	$F(1, 31) = 4.691$	$p = 0.8159$	$F(1,31) = 0.05511$	$p < 0.0001$	$F(1,31) = 20.98$	$p = 0.1738$	$t(31) = 1.768$	$p = 0.0001$	$t(31) = 4.617$
11–6	$p = 0.0045$	$t(33) = 3.052$	$p = 0.0009$	$F(1, 31) = 13.59$	$p = 0.0004$	$F(1,31) = 16.12$	$p < 0.0001$	$F(1, 31) = 24.39$	$p = 0.7329$	$t(31) = 0.9165$	$p < 0.0001$	$t(31) = 5.903$
Il-1β	$p < 0.0001$	$t(33) = 5.210$	$p = 0.2913$	$F(1, 31) = 1.152$	$p = 0.6248$	$F(1, 31) = 0.2440$	$p < 0.0001$	$F(1, 31) = 25.02$	$p = 0.0144$	$t(31) = 2.877$	$p = 0.0005$	$t(31) = 4.158$
iNos	$p = 0.0236$	$t(33) = 2.374$	$p = 0.0235$	$F(1, 31) = 5.679$	$p = 0.0845$	$F(1, 31) = 3.176$	$p = 0.0053$	$F(1, 31) = 8.976$	$p > 0.9999$	$t(31) = 0.4489$	$p = 0.0018$	$t(31) = 3.681$
Arg	$p = 0.0080$	$t(33) = 2.822$	$p = 0.1787$	$F(1,31)= 1.893$	$p = 0.2725$	$F(1, 31) = 1.248$	$p = 0.0043$	$F(1, 31) = 9.509$	$p = 0.4409$	$t(31) = 1.251$	$p = 0.0093$	$t(31) = 3.052$
Fig. 8			Two-way ANOVA						Post-hoc			
			Interaction		Repopulation		TCDD		Control		PLX (Repopulation)	
			P value	Test Stat	P value	Test Stat	P value	Test Stat	P value	Test Stat	P value	Test Stat
Tnf-α			$p = 0.0059$	$F(1, 20) = 9.477$	$p = 0.3386$	$F(1,20) = 0.9613$	$p = 0.0519$	$F(1, 20) = 4.274$	$p = 0.0031$	$t(20) = 3.665$	$p = 0.9719$	$t(20) = 0.7099$
Il-6			$p = 0.0001$	$F(1, 20) = 22.08$	$p = 0.0088$	$F(1, 20) = 8.432$	$p = 0.0046$	$F(1, 20) = 10.16$	$p < 0.0001$	$t(20) = 5.617$	$p = 0.6025$	$t(20) = 1.061$
Il-1β			$p = 0.0002$	$F(1, 20) = 21.06$	$p = 0.0014$	$F(1, 20) = 13.64$	$p = 0.0011$	$F(1, 20) = 14.55$	$p < 0.0001$	$t(20) = 5.985$	$p > 0.9999$	$t(20) = 0.5438$
iNos			$p = 0.0066$	$F(1, 20) = 9.199$	$p = 0.0315$	$F(1, 20) = 5.350$	$p = 0.1417$	$F(1, 20) = 2.341$	$p = 0.0080$	$t(20) = 3.249$	$p = 0.6077$	$t(20) = 1.055$
Arg			$p = 0.0002$	$F(1, 20) = 21.49$	$p = 0.0023$	$F(1, 20) = 12.15$	$p = 0.0011$	$F(1, 20) = 14.47$	$p < 0.0001$	$t(20) = 6.011$	$p > 0.9999$	$t(20) = 0.5842$